The energy between two ions is thus the sum of the coulombic and the repulsive components:

$$U = - \frac{q_1 \cdot q_2}{r} + b.e^{-r/a} \qquad (9.4)$$

In an ionic crystal, formed by an array of negative and positive ions, the lattice energy can be calculated by summing the interactions of each ion with all the other negative and positive ions in the crystal:

$$U = - \frac{1}{2} \sum_i \sum_{j \neq i} \frac{q_i q_j}{r_{ij}} + \frac{1}{2} \, b \sum_i \sum_{j \neq i} e^{-r/a} \qquad (9.5)$$

The factor 1/2 must be introduced because each ion pair is counted twice in the double sum over i and j.

Very accurate calculations of the lattice energy require the inclusion of other factors:

1) the van der Waals forces, due to the interactions between the time-dependent dipoles and quadrupoles, which result from the failure of the centre of the electron cloud to coincide with the nucleus [183]. These forces are proportional to $\frac{1}{r^6}$ and $\frac{1}{r^8}$ for dipole-dipole and dipole-quadrupole interactions respectively, and usually amount to 1 - 2% of the lattice energy, except in the case of highly polarisable ions, where they can be as much as 10 - 15% of the total energy (cf Table 9.1).

2) the zero-point energy, which is given by the ionic vibrations in the crystal at -273K; it is normally very small, and accounts for ~1% of the total energy.

Table 9.1 shows the relative importance of these contributions to the total lattice energy (all energies are expressed in kJ/mol).

TABLE 9.1

Contributions of various components of the lattice energy in alkali halides [kJ/mol]

Compound	Total lattice energy	Electro-static inter-action	Born repulsion	Van der Waals energy	Zero-point energy
LiF	-1013	-1196	+183	-16	+16
NaCl	-767	-862	+100	-13	+8
CsI	-573	-619	+63	-46	+29
AgCl	-846	-875	+146	-121	+4
TlCl	-703	-732	+142	-117	+4

Other contributions to the lattice energy which are not present in all ionic crystals are:

- Crystal field stabilisation energy, due to the splitting of the d orbitals, constitutes a small part of the overall lattice energy of transition metal compounds, and is of the order of a few percent.

- Ordering energy, often less than one percent of the total energy, intervenes when different ions occupy the same crystallographic position but display an orderly distribution, giving rise to a superstructure (cf section 1.2.3.3.i).

As it is evident from the above discussion, the electrostatic energy is the largest single contribution to the total energy of the crystal; for this reason, it is widely accepted as a useful approximation of the lattice energy, and its calculation has attracted considerable interest.

9.3 ELECTROSTATIC ENERGY AND THE MADELUNG CONSTANT

Noting that the electrostatic energy depends solely on the ionic charges and on their spatial distribution, Madelung [184] introduced an adimensional constant for every crystal structure type.

The Madelung constant (α) is a sum of alternately positive and negative terms, which describe the geometrical arrangement of the ionic environment surrounding a particular ion in the structure.

A simple example is the case of NaCl, where the structure can be described as two cubic close-packed arrays of sodium and chloride ions respectively, shifted by half a lattice parameter from one another. Because of the symmetry of NaCl, the ionic environment of the chloride ions is identical to that of the sodium ions, but with opposite charges: the Madelung constant need therefore only be calculated for one ion.

The environment of each sodium ion consists of:

6 Cl^- at a distance r
12 Na^+ at a distance $r.\sqrt{2}$
8 Cl^- at a distance $r.\sqrt{3}$
6 Na^+ at a distance 2.r
24 Cl^- at a distance $r.\sqrt{5}$
etc.

The Madelung energy of the sodium ion is therefore:

$$E_{el} = \frac{6z(-z)e^2}{r} + \frac{12(z^2)e^2}{r\sqrt{2}} + \frac{8z(-z)e^2}{r\sqrt{3}} + \frac{6(z^2)e^2}{2r} + \frac{24z(-z)e^2}{r\sqrt{5}} + \ldots$$

$$= -\frac{z^2e^2}{r}\underbrace{\left(6 - \frac{12}{\sqrt{2}} + \frac{8}{\sqrt{3}} - \frac{6}{2} + \frac{2}{\sqrt{5}} + \ldots\right)}_{\alpha_{NaCl}}$$

where α_{NaCl} = Madelung constant for NaCl-type structures
z = valence
r = interionic distance

In general the coulombic energy for a compound $A_mB_nX_p$ is given by:

$$E_{el} = - \frac{e^2}{r} (m\alpha_A + n\alpha_B + p\alpha_X) \qquad (9.6)$$

where r = characteristic parameter, i.e., shortest interionic distance or lattice parameter.

$\alpha_{A,B,X}$ = partial Madelung constant of the ions A,B,X.

Madelung constants for fairly simple and symmetric structures have been calculated and are widely available in the literature [185]; they can be used for all compounds which crystallise with the same structure, and thus simplify the calculation of the electrostatic energy.

In the case of more complicated structures, it is advisable, and often necessary, to calculate the Madelung energy of each compound individually [186].

Examples are perovskites, where the oxidation state of the ions varies from one compound to another, and spinels, where the oxidation state and the distribution of the cations, as well as the anion positional parameter, must be taken into account.

In order to obtain the Madelung energy of these compounds, it is necessary to evaluate the partial Madelung constant of each ion present in the structure (eq. 9.6); to this purpose, it is convenient to calculate the electrostatic self-potential V_i of each ion site, i.e., the potential at that site after the charge has been removed.

The self-potential is related to the partial Madelung constant by the equation:

$$V_i = - \frac{2\, e^2 \alpha_y(i)}{r \cdot q_i} \qquad (9.7)$$

where V_i = self potential at the ion site

$\alpha_y(i)$ = partial Madelung constant of the ion y in site i

q_i = charge of the ion in site i

The coulombic energy will then be given by the expression:

$$E_{el} = \frac{1}{2} \sum_i n_i q_i V_i \qquad (9.8)$$

where V_i, q_i = as defined above

n_i = number of ions with q_i in site i per formula unit.

Thus, for example, in the case of the spinels $A^{2+}[B^{3+}_2]X_4$, the electrostatic energy will be:

$$E_{(AB_2X_4)} = \frac{1}{2} \left((+2) \cdot V_{8a} + 2 \cdot (+3) \cdot V_{16d} + 4(-2) \cdot V_{32e} \right) \qquad (9.9)$$

Several methods for the evaluation of the self-potentials and hence of the Madelung energy are briefly described in the following section.

9.4 SHORT SURVEY OF METHODS FOR EVALUATING THE MADELUNG ENERGY

The evaluation of the Madelung energy requires the calculation of the electrostatic self-potentials of the lattice.

Two difficulties arise: firstly, the series which express the self-potentials converge slowly, and secondly, they are conditionally convergent, i.e., the result depends on the order with which the terms are arranged [185,187].

Because of this, although a mathematical artifice can transform a slowly converging series into a rapidly converging one, the transformation requires special attention in order to attain a physically meaningful result.

The conditional convergence results from the method of calculation, which is performed over a finite crystal with a well-defined shape, frequently a cube. The faces of the cube are constituted by planes of atoms, which might not be electrically neutral, due to an uneven distribution of the positive and negative ions.

This gives rise to a surface dipole, causing conditional convergence to occur : the final result of the summation will thus depend on the choice of orientation of the cube. Several methods have been suggested in order to solve the problem.

In broad terms, two approaches have been used successfully [185]: the first one involves an appropriate rearrangement of terms followed by a direct summation, e.g, Evjen's method [187]; the second technique consists in a summation which is partially conducted in reciprocal space. The latter system was originally devised by Ewald [188] and has been successfully applied to many structures.

In Evjen's method [187], ions situated on the faces, edges or corners of the unit cell belong to 2, 4 or 8 unit cells respectively; it is therefore necessary to divide their charges by 2, 4 or 8, whilst the charges in the interior of the unit cell are maintained at their real value.

The method is most straightforward for cases where there is no surface dipole, e.g., NaCl; it is less satisfactory for structures where the faces of the unit cell are not neutral, and where the result varies according to the choice of orientation of the cube, e.g., in CsCl.

In the latter case, Evjen [187] assumed that the correct result was the arithmetic mean value of the two different orientations; Dahl [189] has since given a more rigorous explanation, together with an extension of the method which allows an unambiguous computation for all structures.

Ewald's approach is based on an entirely different concept. The crystal is subdivided into Bravais lattices of unit point charges neutralised by a uniform background in order to ensure convergence. The charge distribution is divided into two series. The first one is a set of Gaussian functions normalised to +1 and neutralised by a uniform charge distribution, the second one consists of unit point charges with neutralising Gaussian functions.

Ewald combines the latter series in the direct space with the Fourier transform over the reciprocal lattice of the former series, and thus obtains a rapid and unconditional convergence. Several variations of the method have been formulated, amongst which are Bertaut's [190] and the planewise summation method (PSM): the latter was used in this work and will be briefly described in section 9.5.

9.5 CALCULATION OF MADELUNG ENERGIES BY THE PLANEWISE SUMMATION METHOD (PSM)

The planewise summation method (PSM), which can be considered to be an extension of Ewald's method, was first presented by Nijboer and De Wette in 1957 [191] as a general method for the calculation of lattice sums, with special reference to dipole lattices. A more detailed description was given by De Wette and Schacher in 1965 [192,193].

As in Ewald's method, the principle of the PSM is to attain rapid convergence by combining two sums, i.e., the original summation and an auxiliary function, one of which is taken in the form of

its Fourier transform over the reciprocal lattice. The PSM simplifies Ewald's procedure by choosing the first function in such a manner that an auxiliary function is only necessary for specific conditions, and convergence is attained by transforming the entire sum into Fourier space.

A slab-shaped crystal was found to be advantageous in order to solve the ambiguities caused by conditional convergence. If a_1, a_2, a_3 are the crystallographic primitive vectors and λ_1, λ_2, λ_3 are integers, the position of a sublattice i is given by the expression:

$$r_{\lambda i} = \lambda_1 a_1 + \lambda_2 a_2 + \lambda_3 a_3 \qquad (9.10)$$

A slab-shaped crystal with faces parallel to a_1 and a_2 is chosen. The summation is conducted over λ_1 and λ_2 with a fixed λ_3, and is made to converge by transforming it in Fourier space.

The summations for different values of λ_3 can then be added analytically, and the entire calculation ultimately results in one rapidly converging series over the two-dimensional reciprocal lattice.

However, in certain cases, e.g., when the ion site under calculation is situated in one of the a_1, a_2 planes, it is necessary to include an auxiliary function in the computation for that particular plane; this added complication can be avoided by a judicious choice of the a_1, a_2 planes.

A surface charge distribution is included in the computation, and, by mutual cancelling out of dipole layers, the final electrostatic potentials are shape-independent [192,194].

The PSM has the advantage of being simpler to apply than Ewald's method, it has been further developed by Sholl, Massidda and

Hernando [194-198], with particular reference to the calculation of self-potentials and electrostatic energy in ionic crystals.

The results obtained by the PSM are in agreement with those given by Ewald's method [194].

9.6 LATTICE ENERGY OF SPINELS: A BRIEF SURVEY OF THE LITERATURE

Since the bonding in spinels is largely ionic, it is an acceptable approximation to apply the Born-Mayer model [182] (section 9.2) for the calculation of their lattice energy.

The electrostatic energy of spinels was first calculated by Verwey and Heilmann in 1947 [56], with the Evjen summation method [187], in order to achieve a better understanding of the spinel structure and, in particular, of the cation distribution.

In spinels, the atomic layers in the (100) planes contain an alternate excess of anions and cations, which causes an electric dipole layer to appear at the surface of the cube used for the energy computation.

This dipole is not adequately compensated for by Evjen's method. Verwey et al. [57] assumed the error to be constant, and introduced a systematic correction to their original values, which was estimated by calculating the potential drop across the double layer.

Since then, the advent of more sophisticated computing facilities has made more laborious calculations readily accessible. Several authors [61,62,64,199] have recalculated the Madelung energy of spinels, using a variety of summations generally based on Ewald's method [188], and have obtained comparable results.

The electrostatic energy of spinels varies considerably, and depends on the charge distribution and on the anion positional parameter u; noting this, Popov and Levitskii [64] derived an expression for the self-potentials of the spinel sub-lattices, which are a function of the charge of the tetrahedron and of the u parameter.

The repulsion term in spinels has seldom been evaluated, owing to the lack of compressibility data [38]. Verwey and Heilmann [56] estimated that the repulsive energy amounted to approximately 10% of the electrostatic energy. Furthermore, it was generally accepted that the repulsion term would not vary very much within the class of compounds with a spinel structure, since the structural characteristics are constant and the ionic radii of the cations are similar.

This assumption was recently proven to be correct by Popov and Levitskii [200], who calculated the repulsive energy of binary oxides with the spinel or ilmenite structure. In their study, they showed that the repulsion term does not vary much within an isostructural class of compounds, and is almost independent of the nature of the A cation for a given $[B_2]X_4$ framework. Contrary to previous assumptions, Popov and Levitskii found the repulsive energy of spinels to amount to 20 - 25% of the electrostatic energy.

The same authors evaluated various other factors contributing to the overall lattice energy in a recent study of the thermodynamics of spinel oxides [64,200-202].

Ordering energies were included for superstructures [64], and were found to amount to 1 - 3% of the electrostatic energy, in good agreement with the values obtained previously by de Boer et al. [203].

The van der Waals energy [201] was virtually independent of A within a series AB_2O_4; furthermore, the van der Waals interaction energy amounted to approximately the same value for all AB_2O_4 spinels, in the range of 80 -100 kcal/mol, i.e., 1.5 - 2.0% of the electrostatic energy.

The zero-point energy [202] was found to be negligible, of the order of 0.2% of the electrostatic energy, whereas the stabilisation energy, due to the ligand field splitting of the transition metal d orbitals, makes a much larger contribution, of approximately 5% in the most favourable cases [202]. The latter results were found to be consistent with the stabilisation energy calculated using the MO-LCAO method (cf section 1.2.4.3) [65].

In conclusion, it is observed that the electrostatic interaction energy is not only the largest contribution to the total lattice energy, but it is also the component which varies the most within the entire series of spinel compounds: it is therefore a relevant factor to consider when comparing the reactivity and the structure of different spinels.

9.7 MECHANISM OF LITHIUM INSERTION INTO Mn_3O_4 AND $LiMn_2O_4$

Lithium has been inserted at room temperature into the spinels Mn_3O_4 and $LiMn_2O_4$, both by chemical means, with n-BuLi, and electrochemically, using a Li anode [33].

The structures of $LiMn_3O_4$ and $Li_2Mn_2O_4$ were determined by powder X-ray diffraction [33]. In both compounds the $[B_2]X_4$ spinel framework is maintained during lithiation, and lithium is inserted into the empty octahedral 16c sites. The 16c octahedra are connected to the 8a tetrahedra by common faces (cf section 1.2.5).

In the case of Mn_3O_4, the relatively heavy Mn^{2+} ions occupying the tetrahedral 8a sites migrate through shared faces to the 16c sites at a very early stage of the lithiation process. The inserted lithium and the manganese ions thus share the 16c sites in a random fashion. The reaction mechanism can thus be described by the sequence:

$$(Mn^{2+})_{8a}\,[Mn_2^{3+}]_{16d}O_4$$

$$\downarrow\ x_c\ Li^+$$

$$\{Li^+_{x_c}\}_{16c}(Mn^{+2})_{8a}\,[Mn_2^{2+/3+}]_{16d}O_4$$

$$\downarrow$$

$$\{Li^+_{x_c}Mn^{2+/3+}\}_{16c}[Mn_2^{2+/3+}]_{16d}O_4$$

$$\downarrow\ (1 - x_c)\ Li^+$$

$$\{Li^+Mn^{2+/3+}\}_{16c}[Mn_2^{2+/3+}]_{16d}O_4$$

In $Li[Mn_2]O_4$ the lithiation process is similar, with the inserted lithium occupying the 16c octahedral sites. However, because the lithium ion is small and monovalent, the interaction between the incoming lithium ions in the 16c sites and those already present in the neighbouring 8a sites is considerably less than in $Li_xMn_3O_4$, and a complete migration of the lithium ions from the tetrahedral sites is not observed.

In a recent neutron diffraction study [163], it has been shown that the lithium ions are randomly distributed over the 8a and 16c sites in $Li_2Mn_2O_4$. A similar Li^+ distribution was observed in this work, in the case of $Li_{1.5}V_2O_4$ (chapter 6).

The insertion of lithium in spinels is accompanied by a slight shift of the lattice parameters; in the case of $Li_{1+x}Mn_2O_4$ ($0<x\leq1$) the increasing number of Mn^{3+} ions, obtained by the re-

duction of Mn^{4+} to Mn^{3+} upon insertion of Li^+ ions, is the cause of a Jahn-Teller distortion, and the overall symmetry changes from cubic to tetragonal, as is the case in several Mn^{3+}-containing spinels (section 1.2.3.3.ii)[192].

The exact composition at which the change of the cell constants takes place has not been determined: the single-phase character of the electrochemical lithiation in Mn_3O_4 [33] might suggest that this is a gradual process. In the case of $LiMn_2O_4$, however, the electrochemical curve describing the lithiation of $LiMn_2O_4$ shows a two-phase reaction for $0.1<x<0.8$ in $Li_{1+x}Mn_2O_4$, indicating a more sudden change of structure at $x \approx 0.1$.

9.8 PROGRAM USED FOR CALCULATION

The calculation of the electrostatic energy of $Li_xMn_3O_4$ and $Li_{1+x}Mn_2O_4$ (cubic) was carried out on a Cyber 750 computer using an existing Fortran program [204,205] for the evaluation of electrostatic self-potentials (PLATTSUM).

The program, which is described in refs. 204 and 205, is based on the planewise summation method (cf section 9.5), and in particular on the generalisation of the PSM by Massidda and Hernando [198], applicable to multipole lattices of any symmetry.

The self-potential of each occupied crystallographic position is calculated separately, and the electrostatic energy is then obtained according to equation 9.8. The procedure was repeated for several concentrations of lithium and for each compound.

a) **Input**

The nature and format of the input are given in ref. 204; however, certain points will be repeated here for greater clarity.

The first line contains four parameters related to the computation. In this work, the following values were assigned:

NSUM = 1 000 (maximum number of terms included in the calculation for each data set)

NDATAM = 80 (maximum number of data sets)

EPS = 10^{-10} (maximum allowed relative error)

JMIN = 5.10^{-2} (area surrounding the field-point, i.e., the site under calculation, where convergence is too slow)

The second line of the input file consists of the cell constants a, b, c (in Å) and the crystallographic angles α, β, γ (in degrees). The rest of the file consists of sets of two cards, each set describing an ion in the unit cell (i.e., a sublattice): the first card consists of the fractional coordinates of the field point multiplied by (-1), and those of the sublattice which is being considered:

$$-x_o \quad -y_o \quad -z_o \qquad x_s \quad y_s \quad z_s$$

Every occupied site must be described in full, i.e., with its fractional coordinates, since the program makes no provision for symmetry or equivalent positions.

The second card of each data set contains the program commands and the charge of the sublattice.

The program commands are nine logical constants: the first five specify the type of calculation, in this case the potential of a point-charge sublattice. The next three constants define the orientation of the slab-shaped crystal, abc, bca or cab, i.e., the plane in which the calculations are performed. As it was

mentioned in section 9.5, the choice of orientation of the a_1, a_2 axes can simplify the computation. In practice, the best choice is ensured by the program which detects any errors and then prints a message in the output.

The ninth logical command serves to indicate the end of the program.

b) **Output**

A complete printout of the output is reproduced in ref. 204 with a few comments which make any further explanation superfluous.

It must, however, be mentioned that the self-potentials obtained already include the factor 0.5 of equation 9.8; the electrostatic energy is therefore calculated according to the simplified expression:

$$E_{el} = \sum n_i q_i V_i \qquad (9.11)$$

9.9 DATA FOR THE EVALUATION OF THE ELECTROSTATIC ENERGIES OF $Li_xMn_3O_4$ AND $Li_{1+x}Mn_2O_4$ ($0<x<1$)

The space group, lattice parameters and anion fractional coordinates of the reactants and of the final products are listed in Table 9.2.

Equivalent positions of the space groups Fd3m and $I4_1/amd$ were used according to ref. 208, with the origin at the centre ($\bar{3}m$ for Fd3m and 2/m for $I4_1/amd$).

In order to simplify the discussion, the $I4_1/amd$ positions will be described using the Fd3m notation in this chapter; Table 9.3 gives the corresponding sites in the two space groups [50].

TABLE 9.2

Structural data of reactants and lithiated products

Compound	Space Group	Lattice Parameters [A]	Anion Fractional Coordinates	Ref
Mn_3O_4	$I4_1/amd(D_{4h}^{19})$	a=5.763 c=9.456	(0;0.464;0.259)	206 207
$LiMn_3O_4$	$I4_1/amd(D_{4h}^{19})$	a=6.022 c=9.011	(0;0.487;0.253)	33
$LiMn_2O_4$	$Fd3m(O_h^7)$	a=8.246	(0.259;0.259;0.259)	168
$Li_2Mn_2O_4$	$I4_1/amd(D_{4h}^{19})$	a=5.662 c=9.9274	(0;0.487;0.252)	33

TABLE 9.3

Corresponding sites in Fd3m and $I4_1/amd$ [50]

DESCRIPTION	Fd3m (Z = 8)	$I4_1/amd$ (Z = 4)
A sites	8a	4a
Empty octahedral sites	16c	8c
B sites	16d	8d
Anion sites	32e	16h

When two or more types of ion occupy the same site, a random distribution was assumed, and an average charge was used in the calculation.

Before undertaking any computations on the compounds $Li_xMn_3O_4$ and $Li_{1+x}Mn_2O_4$, the program was tested by calculating the self-potentials and the electrostatic energy of the spinel $Mg[Al_2]O_4$. The results obtained were in fairly good agreement with the values indicated by other authors [64].

9.10 RESULTS AND DISCUSSION

With the aim of improving our understanding of the lithiation process, electrostatic energy calculations were carried out for two different models: in both cases, the incoming lithium occupies the octahedral 16c sites, which are empty in spinels.

In model 1, the ions situated in the tetrahedral 8a positions remain fixed; in model 2, the ions in 8a have migrated to the face-sharing 16c positions, which they share with the inserted lithium in a random distribution. The former model is an approximation of the structure found experimentally for $Li_2Mn_2O_4$, where about one-third of the lithium ions occupy the 8a sites, and the remaining two-thirds the 16c sites, showing a final overall displacement of only one-third of the original lithium ions from the 8a to the 16c positions [163]. Model 2 reflects the structure of $LiMn_3O_4$, where all the manganese ions in the 8a sites migrate to the 16c sites [33].

Calculations were carried out for the full range of x in $Li_{1+x}Mn_2O_4$ and $Li_xMn_3O_4$ ($0<x<1$) using the cell parameters of the parent compounds $LiMn_2O_4$ and Mn_3O_4; identical computations were done with the cell constants and oxygen positional parameters of $Li_2Mn_2O_4$ and $LiMn_3O_4$, for the higher values of x.

The electrostatic energy of the final compound $Li_2Mn_2O_4$ was also calculated with a random distribution of the lithium ions over the 8a and the 16c sites. The charges at the individual sites and

the calculated self-potentials for $Li_xMn_3O_4$ and $Li_{1+x}Mn_2O_4$ ($0 \leq x \leq 1$), according to Models 1 and 2, are given in section "a" of Tables 9.4 - 9.7.

The electrostatic energy for these structures is listed in section "b" of Tables 9.4 - 9.7, together with the individual contributions to the total coulombic energy of the atoms located in the 8a, 16c, 16d and 32e sites.

The data obtained for a random distribution of lithium in $Li_2Mn_2O_4$ are presented in Table 9.8.

Several graphic representations of the variation of energy and self-potential as a function of the composition are given in Figs 9.1 - 9.11.

Although the use of the structural parameters of the final compounds $LiMn_3O_4$ and $Li_2Mn_2O_4$ for the higher values of x often alters the potentials and the energies in a significant manner, especially in the case of $Li_{1+x}Mn_2O_4$, where the structure changes from cubic to tetragonal symmetry, the trends are comparable to those observed using the parameters of the parent compounds.

Since most of the discussion and conclusions are based on the relative differences of energy and potentials, and not on the absolute values, the analysis which follows will be based on results obtained for the parent compound structure, unless otherwise specified.

a) **Electrostatic energy and relative stability**

Examination of the electrostatic energies obtained for the compounds $Li_xMn_3O_4$ and $Li_{1+x}Mn_2O_4$ (cf Tables 9.4 - 9.8, Figs 9.1 - 9.2) immediately reveals the metastable character of these products:

$\Delta E\ (Mn_3O_4 \xrightarrow{Li} LiMn_3O_4) \approx 1160$ kcal/mol

$\Delta E\ (LiMn_2O_4 \xrightarrow{Li} Li_2Mn_2O_4) \approx 1170$ kcal/mol

Many ambient-temperature insertion compounds, e.g., $Li_xV_2O_5$ ($0<x<1$) [209], Li_xMoO_3 ($x\leq2$) [13,19] and $Li_{1+x}Fe_5O_8$ ($x\approx2$) [31], have been shown to be metastable and to convert to more stable structures of the same or similar composition when heated. Other insertion compounds have been found to decompose to oxy-salts and lower oxides [210], e.g., Li_xWO_3 ($x<1$) [211].

Surprisingly, the structures obtained experimentally proved to be the least stable according to the Madelung energy calculations: in the case of $LiMn_3O_4$ the structure where the manganese ions remain in the tetrahedral sites (model 1) was predicted to be the most stable, whereas the preferred structure of $Li_2Mn_2O_4$ implied the migration of all lithium ions to the octahedral 16c sites (model 2), contrary to experimental results (section 9.7).

It is generally accepted that the preferred structure will have the lowest Madelung energy; this assumption did not prove correct in this case: possible reasons for this will be discussed in section 9.11.

However, the electrostatic energies calculated for the various lithiation mechanisms differ from one another by only 50 - 70 kcal/mol ($\Delta\Delta E$) for both $LiMn_3O_4$ and $Li_2Mn_2O_4$ (Figs 9.1, 9.2), suggesting that other contributions to the lattice energy may play a decisive role (section 9.11).

Although the lithium insertion mechanism cannot be explained by a simple Madelung energy model (as it has previously been

$\Delta E\ (Mn_3O_4 \xrightarrow{Li} LiMn_3O_4) \approx 1160$ kcal/mol

$\Delta E\ (LiMn_2O_4 \xrightarrow{Li} Li_2Mn_2O_4) \approx 1170$ kcal/mol

Many ambient-temperature insertion compounds, e.g., $Li_xV_2O_5$ ($0<x\leq1$) [209], Li_xMoO_3 ($x\leq2$) [13,19] and $Li_{1+x}Fe_5O_8$ ($x\approx2$) [31], have been shown to be metastable and to convert to more stable structures of the same or similar composition when heated. Other insertion compounds have been found to decompose to oxy-salts and lower oxides [210], e.g., Li_xWO_3 ($x<1$) [211].

Surprisingly, the structures obtained experimentally proved to be the least stable according to the Madelung energy calculations: in the case of $LiMn_3O_4$ the structure where the manganese ions remain in the tetrahedral sites (model 1) was predicted to be the most stable, whereas the preferred structure of $Li_2Mn_2O_4$ implied the migration of all lithium ions to the octahedral 16c sites (model 2), contrary to experimental results (section 9.7).

It is generally accepted that the preferred structure will have the lowest Madelung energy; this assumption did not prove correct in this case: possible reasons for this will be discussed in section 9.11.

However, the electrostatic energies calculated for the various lithiation mechanisms differ from one another by only 50 - 70 kcal/mol ($\Delta\Delta E$) for both $LiMn_3O_4$ and $Li_2Mn_2O_4$ (Figs 9.1, 9.2), suggesting that other contributions to the lattice energy may play a decisive role (section 9.11).

Although the lithium insertion mechanism cannot be explained by a simple Madelung energy model (as it has previously been

suggested [33]), nevertheless some useful information can be obtained from the examination of the changes of the self-potentials and energies of each crystallographic site (Tables 9.4 - 9.8, Figs 9.3 - 9.10).

As it might be anticipated, the self-potentials of the 16d and 32e sites undergo very little change during the entire lithiation process (Figs 9.3 - 9.6); in terms of electrostatic energy, both sites are subject to destabilisation, which is slightly more pronounced in model 2.

The self-potentials and energies in the 8a and 16c sites (Tables 9.4 - 9.8, Figs 9.7 - 9.10) of Models 1 and 2 differ quite considerably; this is due to the close proximity of these sites, which causes strong interactions between the ions situated in them.

b) **Self-potentials of the 8a and 16c sites**

The self-potentials of the 8a sites (in both $Li_xMn_3O_4$ and $Li_{1+x}Mn_2O_4$) increase sharply as the lithiation progresses, confirming the destabilising effect of the incoming lithium cations in the adjacent 16c sites (Figs 9.7 - 9.8).

The self-potentials in the 16c sites, calculated for the two models, differ widely: in model 1, where there is a continuous presence of ions in the face-sharing 8a sites, the self-potential is very high, whereas in model 2, where the 8a sites are empty, the potential of the 16c sites is closer to the values found for the 8a and 16d sites in the parent compounds. In both cases, the stability of the ions in the 16c sites increases slightly as the insertion progresses, and the change of the structural parameters in the end-products has a stabilising effect on the self-potentials of approximately 2 Volts.

Thus, according to model 1, the self-potential of the 16c sites is almost prohibitive for cations in $Li_xMn_3O_4$, with values ranging from 0V to -1V, whereas in model 2 it amounts to approximately -9V, creating an energetically more favourable situation for the ions in these sites.

This is not true in the case of $Li_{1+x}Mn_2O_4$: the self-potential in the 16c sites has a value of approximately -6V and -11V for models 1 and 2 respectively; although these figures appear to favour model 2, they do not rule out the possibility of model 1 as in the case of $Li_xMn_3O_4$.

c) **Electrostatic energy of the 8a and 16c sites**

Similar conclusions are reached upon examination of the contributions to the electrostatic energy of the 8a and 16c sites (Figs 9.9 - 9.10). For $Li_xMn_3O_4$, according to model 1, there is a destabilisation of the 8a sites by ~8 eV, which is hardly compensated by the stabilisation of ~1 eV of the 16c sites; in model 2, where there is no destabilising effect on the part of the 8a sites, the ions in the 16c sites increase the relative stability by ~6.5 eV. Thus, despite the fact that the total electrostatic energy calculations do not agree with the structure of $LiMn_3O_4$ obtained experimentally, the latter is partly explained by the values of the self-potentials and energies of the 8a and 16c sites.

The choice of mechanism is not as clear for $Li_{1+x}Mn_2O_4$, where the destabilisation of the 8a sites is more than compensated by the increasing stability of the 16c sites in model 1; an even greater stability of the latter is observed in model 2.

In both compounds, the global destabilisation of the entire structure comes mainly from the loss of stability in the

$[B_2]X_4$ framework, as the energy of both the 16d and the 32e sites increases.

d) **Cation-cation interaction energy**

Since the interactions between the 8a and 16c cations would appear a priori to be the major factor responsible for the mechanism of lithium insertion, the electrostatic energy due solely to the cation-cation interactions might be expected to be significant.

Calculations of the coulombic cation-cation interactions were carried out by omitting all the anions from the structure; results are listed in Tables 9.9 - 9.13 and illustrated in Fig. 9.11. As in the case of the total electrostatic energy, there is little difference (~100 kcal/mol) between the final structures obtained according to the different models.

The more stable structure for $LiMn_3O_4$ agrees with the experimental data, although model 1 is predicted as the preferred pathway for $Li_xMn_3O_4$, where $0<x\leq0.8$, in contradiction with observation.

The predicted structure for $Li_2Mn_2O_4$ conflicts with experimental findings; however, neither model can be ruled out, as the cation-cation interactions in the two cases are very similar for the entire range of x, and differ by 0 -100 kcal/mol.

Although the coulombic cation-cation interaction energies for both models are similar for the composition $LiMn_3O_4$, this is not true for lower values of x in $Li_xMn_3O_4$ (Fig. 9.11): if model 1 is followed, the destabilising effect increases steadily, whereas in model 2 there is a sudden increase of the interactions between cations, and the energy remains almost constant thereafter.

The lithiation of Mn_3O_4 is known to take place initially according to model 1; at a critical value of x in $Li_xMn_3O_4$ ($x \approx 0.04$), Mn^{2+} migrates from the 8a to the 16c sites, and model 2 is then followed until completion of the reaction.

It may be seen in Fig. 9.11, and to a lesser extent in Fig. 9.1, that although the sudden change of mechanism initially involves a sharp increase in energy, the subsequent lithiation hardly affects the coulombic energy due to the interactions between cations, which remains virtually constant.

This pathway is reminiscent of the Hammond postulate [212] which predicts that the transition states of highly endothermic processes will resemble the products.

If the intermediate compounds $Li_xMn_3O_4$ ($0<x<1$) are considered to be the transition states, then they would be expected to have a similar structure to the product, $LiMn_3O_4$: the conversion would then involve only a lesser change in structure and energy, and the reaction would thus be facilitated.

TABLE 9.4

a) Charges and self-potentials of $Li_xMn_3O_4$ ($0<x<1$) according to model 1

x	Q_{8a}	Q_{16c}	Q_{16d}	V_{8a} [Volts]	V_{16c} [Volts]	V_{16d} [Volts]	V_{32e} [Volts]
0.00	+2.000	-	+3.000	-12.799	-7.706	-18.231	+14.018
0.02	+2.000	+0.010	+2.990	-12.716	-0.776	-18.226	+13.999
0.06	+2.000	+0.030	+2.970	-12.550	-0.785	-18.216	+13.961
0.10	+2.000	+0.050	+2.950	-12.384	-0.795	-18.206	+13.922
0.25	+2.000	+0.125	+2.875	-11.761	-0.815	-18.170	+13.778
0.50	+2.000	+0.250	+2.750	-10.722	-0.892	-18.109	+13.538
0.75	+2.000	+0.375	+2.625	-9.684	-0.953	-18.048	+13.297
1.00	+2.000	+0.500	+2.500	-8.646	-1.014	-17.987	+13.057
0.75*	+2.000	+0.375	+2.625	-12.692	-2.931	-14.497	+12.659
1.00*	+2.000	+0.500	+2.500	-11.645	-2.959	-14.468	+12.575

($Q_{32e} = -2.000$)

TABLE 9.4

b) Total electrostatic energy of $Li_xMn_3O_4$ ($0<x<1$) and contributions from each site (model 1)

x	E_{8a} [eV]	E_{16c} [eV]	E_{16d} [eV]	E_{32e} [eV]	E_{tot} [eV]	E_{tot} [kcal/mol]
0.00	-25.60	-	-109.38	-112.15	-247.13	-5699
0.02	-25.43	-0.02	-108.99	-111.99	-246.43	-5683
0.06	-25.10	-0.05	-108.20	-111.68	-245.03	-5650
0.10	-24.77	-0.08	-107.42	-111.38	-243.65	-5619
0.25	-23.52	-0.20	-104.48	-110.22	-238.42	-5498
0.50	-21.44	-0.45	-99.60	-108.30	-229.79	-5299
0.75	-19.37	-0.72	-94.75	-106.38	-221.22	-5101
1.00	-17.29	-1.01	-89.94	-104.45	-212.69	-4905
0.75*	-25.38	-2.20	-76.11	-101.27	-204.96	-4726
1.00*	-23.31	-2.96	-72.34	-100.60	-199.21	-4594

* Calculated using structural parameters of $LiMn_3O_4$.

TABLE 9.5

a) Charges and self-potentials of $Li_xMn_3O_4$ ($0<x<1$) according to model 2

x	Q_{16c}	Q_{16d}	V_{16c} [Volts]	V_{16d} [Volts]	V_{32e} [Volts]
0.02	+1.340	+2.660	-8.910	-17.244	+13.466
0.06	+1.353	+2.647	-8.917	-17.238	+13.441
0.10	+1.367	+2.633	-8.923	-17.231	+13.415
0.20	+1.400	+2.600	-8.939	-17.215	+13.309
0.40	+1.467	+2.533	-8.972	-17.183	+13.223
0.60	+1.533	+2.467	-9.004	-17.150	+13.095
0.80	+1.600	+2.400	-9.037	-17.118	+12.966
1.00	+1.667	+2.333	-9.069	-17.085	+12.838
0.80*	+1.600	+2.400	-10.746	-13.600	+12.264
1.00*	+1.667	+2.333	-10.761	-13.585	+12.220

($Q_{32e} = -2.000$)

TABLE 9.5

b) Total electrostatic energy of $Li_xMn_3O_4$ ($0<x\leq1$) and contributions from each site (model 2)

x	E_{16c} [eV]	E_{16d} [eV]	E_{32e} [eV]	E_{tot} [eV]	E_{tot} [kcal/mol]
0.02	-23.88	-91.74	-107.73	-223.35	-5151
0.06	-24.14	-91.25	-107.53	-222.92	-5141
0.10	-24.39	-90.75	-107.32	-222.46	-5130
0.20	-25.03	-89.60	-106.77	-221.40	-5106
0.40	-26.32	-87.06	-105.78	-219.16	-5054
0.60	-27.61	-84.61	-104.76	-216.98	-5004
0.80	-28.92	-82.16	-103.73	-214.81	-4954
1.00	-30.23	-79.73	-102.71	-212.67	-4904
0.80*	-34.39	-65.28	-98.11	-197.78	-4561
1.00*	-35.87	-63.40	-97.76	-197.03	-4543

* Calculated using structural parameters of $LiMn_3O_4$.

TABLE 9.6

a) Charges and self-potentials of $Li_{1+x}Mn_2O_4$ ($0<x\leq1$) according to model 1

x	Q_{8a}	Q_{16c}	Q_{16d}	V_{8a} [Volts]	V_{16c} [Volts]	V_{16d} [Volts]	V_{32e} [Volts]
0.00	+1.000	-	+3.500	-14.522	-5.821	-18.930	+16.075
0.05	+1.000	+0.025	+3.475	-14.301	-5.850	-18.901	+16.045
0.10	+1.000	+0.050	+3.450	-14.080	-5.879	-18.872	+16.016
0.20	+1.000	+0.100	+3.400	-13.637	-5.936	-18.815	+15.958
0.40	+1.000	+0.200	+3.300	-12.752	-6.051	-18.700	+15.843
0.60	+1.000	+0.300	+3.200	-11.867	-6.166	-18.585	+15.725
0.80	+1.000	+0.400	+3.100	-10.983	-6.281	-18.470	+15.608
1.00	+1.000	+0.500	+3.000	-10.098	-6.396	-18.355	+15.492
0.60*	+1.000	+0.300	+3.200	-12.894	-7.255	-16.043	+14.188
0.80*	+1.000	+0.400	+3.100	-12.089	-7.327	-15.971	+14.122
1.00*	+1.000	+0.500	+3.000	-11.285	-7.400	-15.898	+14.055

(Q_{32e} = - 2.000)

TABLE 9.6

b) Total electrostatic energy of $Li_{1+x}Mn_2O_4$ ($0<x<1$) and contributions from each site (model 1)

x	E_{8a} [eV]	E_{16c} [eV]	E_{16d} [eV]	E_{32e} [eV]	E_{tot} [eV]	E_{tot} [kcal/mol]
0.00	-14.52	-	-132.51	-128.60	-275.63	-6356
0.05	-14.30	-0.29	-131.36	-128.36	-274.31	-6326
0.10	-14.08	-0.59	-130.22	-128.13	-273.02	-6296
0.20	-13.64	-1.19	-127.94	-127.66	-270.43	-6236
0.40	-12.75	-2.42	-123.42	-126.75	-265.34	-6119
0.60	-11.87	-3.70	-118.94	-125.80	-260.31	-6003
0.80	-10.98	-5.03	-114.52	-124.87	-255.40	-5890
1.00	-10.10	-6.40	-110.13	-123.93	-250.56	-5778
0.60*	-12.89	-4.35	-102.68	-113.51	-233.43	-5383
0.80*	-12.09	-5.86	-99.02	-112.97	-229.94	-5302
1.00*	-11.29	-7.40	-95.39	-112.44	-226.52	-5224

* Calculated using structural parameters of $Li_2Mn_2O_4$.

TABLE 9.7

a) Charges and self-potentials of $Li_{1+x}Mn_2O_4$ ($0<x<1$) according to model 2

x	Q_{16c}	Q_{16d}	V_{16c} [Volts]	V_{16d} [Volts]	V_{32e} [Volts]
0.05	+0.525	+3.475	-10.566	-18.618	+15.984
0.10	+0.550	+3.450	-10.594	-18.589	+15.955
0.20	+0.600	+3.400	-10.652	-18.532	+15.897
0.40	+0.700	+3.300	-10.767	-18.417	+15.780
0.60	+0.800	+3.200	-10.882	-18.302	+15.664
0.80	+0.900	+3.100	-10.996	-18.187	+15.547
1.00	+1.000	+3.000	-11.111	-18.072	+15.431
0.60*	+0.800	+3.200	-11.250	-15.653	+14.132
0.80*	+0.900	+3.100	-11.322	-15.580	+14.066
1.00*	+1.000	+3.000	-11.395	-15.508	+13.999

(Q_{8a} = 0.00, Q_{32e} = -2.00)

TABLE 9.6

b) Total electrostatic energy of $Li_{1+x}Mn_2O_4$ ($0<x<1$) and contributions from each site (model 1)

x	E_{8a} [eV]	E_{16c} [eV]	E_{16d} [eV]	E_{32e} [eV]	E_{tot} [eV]	E_{tot} [kcal/mol]
0.00	-14.52	-	-132.51	-128.60	-275.63	-6356
0.05	-14.30	-0.29	-131.36	-128.36	-274.31	-6326
0.10	-14.08	-0.59	-130.22	-128.13	-273.02	-6296
0.20	-13.64	-1.19	-127.94	-127.66	-270.43	-6236
0.40	-12.75	-2.42	-123.42	-126.75	-265.34	-6119
0.60	-11.87	-3.70	-118.94	-125.80	-260.31	-6003
0.80	-10.98	-5.03	-114.52	-124.87	-255.40	-5890
1.00	-10.10	-6.40	-110.13	-123.93	-250.56	-5778
0.60*	-12.89	-4.35	-102.68	-113.51	-233.43	-5383
0.80*	-12.09	-5.86	-99.02	-112.97	-229.94	-5302
1.00*	-11.29	-7.40	-95.39	-112.44	-226.52	-5224

* Calculated using structural parameters of $Li_2Mn_2O_4$.

TABLE 9.7

a) Charges and self-potentials of $Li_{1+x}Mn_2O_4$ ($0<x<1$) according to model 2

x	Q_{16c}	Q_{16d}	V_{16c} [Volts]	V_{16d} [Volts]	V_{32e} [Volts]
0.05	+0.525	+3.475	-10.566	-18.618	+15.984
0.10	+0.550	+3.450	-10.594	-18.589	+15.955
0.20	+0.600	+3.400	-10.652	-18.532	+15.897
0.40	+0.700	+3.300	-10.767	-18.417	+15.780
0.60	+0.800	+3.200	-10.882	-18.302	+15.664
0.80	+0.900	+3.100	-10.996	-18.187	+15.547
1.00	+1.000	+3.000	-11.111	-18.072	+15.431
0.60*	+0.800	+3.200	-11.250	-15.653	+14.132
0.80*	+0.900	+3.100	-11.322	-15.580	+14.066
1.00*	+1.000	+3.000	-11.395	-15.508	+13.999

(Q_{8a} = 0.00, Q_{32e} = -2.00)

TABLE 9.7

b) Total electrostatic energy of $Li_{1+x}Mn_2O_4$ ($0<x<1$) and contributions from each site (model 2)

x	E_{16c} [eV]	E_{16d} [eV]	E_{32e} [eV]	E_{tot} [eV]	E_{tot} [kcal/mol]
0.05	-11.09	-129.39	-127.87	-268.36	-6188
0.10	-11.65	-128.26	-127.64	-267.56	-6170
0.20	-12.72	-126.01	-127.18	-265.91	-6132
0.40	-15.07	-121.55	-126.24	-262.87	-6062
0.60	-17.41	-117.13	-125.31	-259.85	-5992
0.80	-19.79	-112.76	-124.38	-256.93	-5925
1.00	-22.22	-108.43	-123.45	-254.10	-5860
0.60*	-18.00	-100.18	-113.06	-231.24	-5332
0.80*	-20.38	-96.60	-112.06	-229.50	-5292
1.00*	-22.79	-93.05	-111.99	-227.83	-5254

* Calculated using structural parameters of $Li_2Mn_2O_4$.

TABLE 9.8

a) Charges and self-potentials of $Li_2Mn_2O_4$ (random distribution of lithium in the 8a and 16c sites)

x	Q_{8a}	Q_{16c}	Q_{16d}	V_{8a} [Volts]	V_{16c} [Volts]	V_{16d} [Volts]	V_{32e} [Volts]
1.0	0.667	0.667	3.0	-8.021	-7.968	-18.261	+15.471
1.0*	0.667	0.667	3.0	-9.576	-8.732	-15.768	+14.036

b) Electrostatic energy of $Li_2Mn_2O_4$ and contributions from each site (random distribution)

x	E_{8a} [eV]	E_{16c} [eV]	E_{16d} [eV]	E_{32e} [eV]	E_{tot} [eV]	E_{tot} [kcal/mol]
1.0	-5.35	-10.62	-109.57	-123.77	-249.31	-5749
1.0*	-6.38	-11.64	-94.61	-112.29	-224.92	-5187

* Calculated using structural parameters of $Li_2Mn_2O_4$.

TABLE 9.9

Cation-cation interactions in $Li_xMn_3O_4$ ($0<x<1$) (Model 1)

a) Charges and self-potentials

x	Q_{8a}	Q_{16c}	Q_{16d}	V_{8a} [Volts]	V_{16c} [Volts]	V_{16d} [Volts]
0.00	+2.00	-	+3.000	-23.926	-11.490	-21.259
0.04	+2.00	+0.020	+2.980	-23.760	-11.500	-21.249
0.10	+2.00	+0.050	+2.950	-23.511	-11.515	-21.235
0.25	+2.00	+0.125	+2.875	-22.887	-11.551	-21.198
0.50	+2.00	+0.250	+2.750	-21.849	-11.612	-21.137
0.75	+2.00	+0.375	+2.625	-20.911	-11.673	-21.076
1.00	+2.00	+0.500	+2.500	-19.772	-11.734	-21.015
1.00*	+2.00	+0.500	+2.500	-19.175	-11.465	-20.305

b) Energy (E_{cc}) due to the cation-cation interactions, and contributions of each site

x	E_{8a} [eV]	E_{16c} [eV]	E_{16d} [eV]	E_{cc} [eV]	E_{cc} [kcal/mol]
0.00	-47.85	-	-127.55	-175.40	-4045
0.04	-47.52	-0.46	-126.65	-174.63	-4027
0.10	-47.02	-1.15	-125.07	-173.24	-3995
0.25	-45.77	-2.89	-121.89	-170.55	-3933
0.50	-43.70	-5.81	-116.25	-165.76	-3822
0.75	-41.62	-8.75	-110.65	-161.03	-3713
1.00	-39.54	-11.73	-105.08	-156.35	-3606
1.00*	-38.35	-11.47	-101 52	-151.34	-3490

* Calculated using structural parameters of $LiMn_3O_4$.

TABLE 9.10

Cation-cation interactions in $Li_xMn_3O_4$ ($0<x\leq1$) (Model 2)

a) Charges and self-potentials

x	Q_{16c}	Q_{16d}	V_{16c} [Volts]	V_{16d} [Volts]
0.04	+1.347	+2.653	-19.633	-20.269
0.10	+1.367	+2.633	-19.643	-20.260
0.20	+1.400	+2.600	-19.658	-20.243
0.40	+1.467	+2.533	-19.691	-20.211
0.80	+1.600	+2.400	-19.756	-20.146
1.00	+1.667	+2.333	-19.789	-20.113
1.00*	+1.667	+2.333	-19.268	-19.422

(Q_{8a} = 0.0)

b) Energy (E_{cc}) due to the cation-cation interactions, and contributions of each site

x	E_{16c} [eV]	E_{16d} [eV]	E_{cc} [eV]	E_{cc} [kcal/mol]
0.04	-52.88	-107.56	-160.44	-3700
0.10	-53.73	-106.70	-160.43	-3700
0.20	-55.05	-105.27	-160.31	-3697
0.40	-57.76	-102.40	-160.16	-3693
0.80	-63.22	-96.70	-159.92	-3688
1.00	-65.96	-93.86	-159.82	-3686
1.00*	-64.23	-90.63	-154.86	-3571

*Calculated using structural parameters of $LiMn_3O_4$.

TABLE 9.11

Cation-cation interactions in $Li_{1+x}Mn_2O_4$ (0<x<1) (Model 1)

a) Charges and self-potentials

x	Q_{8a}	Q_{16c}	Q_{16d}	V_{8a} [Volts]	V_{16c} [Volts]	V_{16d} [Volts]
0.00	+1.00	-	+3.500	-23.921	-15.709	-24.153
0.05	+1.00	+0.025	+3.475	-23.700	-15.737	-24.125
0.10	+1.00	+0.050	+3.450	-23.479	-15.766	-24.039
0.20	+1.00	+0.100	+3.400	-23.036	-15.823	-24.125
0.40	+1.00	+0.200	+3.300	-22.151	-15.938	-23.924
0.80	+1.00	+0.400	+3.100	-20.382	-16.168	-23.694
1.00	+1.00	+0.500	+3.000	-19.497	-16.283	-23.579
1.00*	+1.00	+0.500	+3.000	-18.884	-15.447	-21.284

b) Energy (E_{cc}) due to the cation-cation interactions, and contributions of each site

x	E_{8a} [eV]	E_{16c} [eV]	E_{16d} [eV]	E_{cc} [eV]	E_{cc} [kcal/mol]
0.00	-23.92	-	-169.07	-192.99	-4450
0.05	-23.79	-0.79	-167.67	-192.16	-4431
0.10	-23.48	-1.58	-166.26	-191.32	-4412
0.20	-23.04	-3.16	-163.46	-189.66	-4374
0.40	-22.15	-6.38	-157.90	-186.42	-4299
0.80	-20.38	-12.93	-146.90	-180.22	-4156
1.00	-19.50	-16.28	-141.47	-177.25	-4088
1.00*	-18.88	-15.45	-127.71	-162.04	-3737

*Calculated using structural parameters of $Li_2Mn_2O_4$.

TABLE 9.12

Cation-cation interactions in $Li_{1+x}Mn_2O_4$ ($0<x<1$) (Model 2)

a) Charges and self-potentials

x	Q_{16c}	Q_{16d}	V_{16c} [Volts]	V_{16d} [Volts]
0.05	+0.525	+3.475	-20.453	-23.813
0.10	+0.550	+3.450	-20.482	-23.755
0.20	+0.600	+3.400	-20.539	-23.842
0.40	+0.700	+3.300	-20.654	-23.641
0.80	+0.900	+3.100	-20.884	-23.411
1.00	+1.000	+3.000	-20.998	-23.296
1.00*	+1.000	+3.000	-19.442	-20.893

b) Energy (E_{cc}) due to the cation-cation interactions, and contributions of each site

x	E_{16c} [eV]	E_{16d} [eV]	E_{cc} [eV]	E_{cc} [kcal/mol]
0.05	-21.48	-165.70	-187.17	-4316
0.10	-22.53	-164.31	-186.84	-4309
0.20	-24.65	-161.54	-186.18	-4293
0.40	-28.92	-156.03	-184.94	-4265
0.80	-37.59	-145.15	-182.74	-4214
1.00	-42.00	-139.76	-181.77	-4192
1.00*	-38.88	-125.36	-164.24	-3788

*Calculated using structural parameters of $Li_2Mn_2O_4$.

TABLE 9.13

Cation-cation interactions of $Li_2Mn_2O_4$ with a random distribution of lithium in the 8a and 16c sites

a) Charges and self-potentials

x	Q_{8a}	Q_{16c}	Q_{16d}	V_{8a} [Volts]	V_{16c} [Volts]	V_{16d} [Volts]
1.00	+0.667	+0.667	+3.000	-17.420	-17.85	-23.48
1.00*	+0.667	+0.667	+3.000	-17.180	-16.78	-21.15

b) Energy (E_{cc}) due to the cation-cation interactions and contributions of each site

x	E_{8a} [eV]	E_{16c} [eV]	E_{16d} [eV]	E_{cc} [eV]	E_{cc} [kcal/mol]
1.00	-11.61	-23.81	-140.91	-176.33	-4066
1.00*	-11.45	-22.37	-126.92	-160.75	-3707

*Calculated using structural parameters of $Li_2Mn_2O_4$.

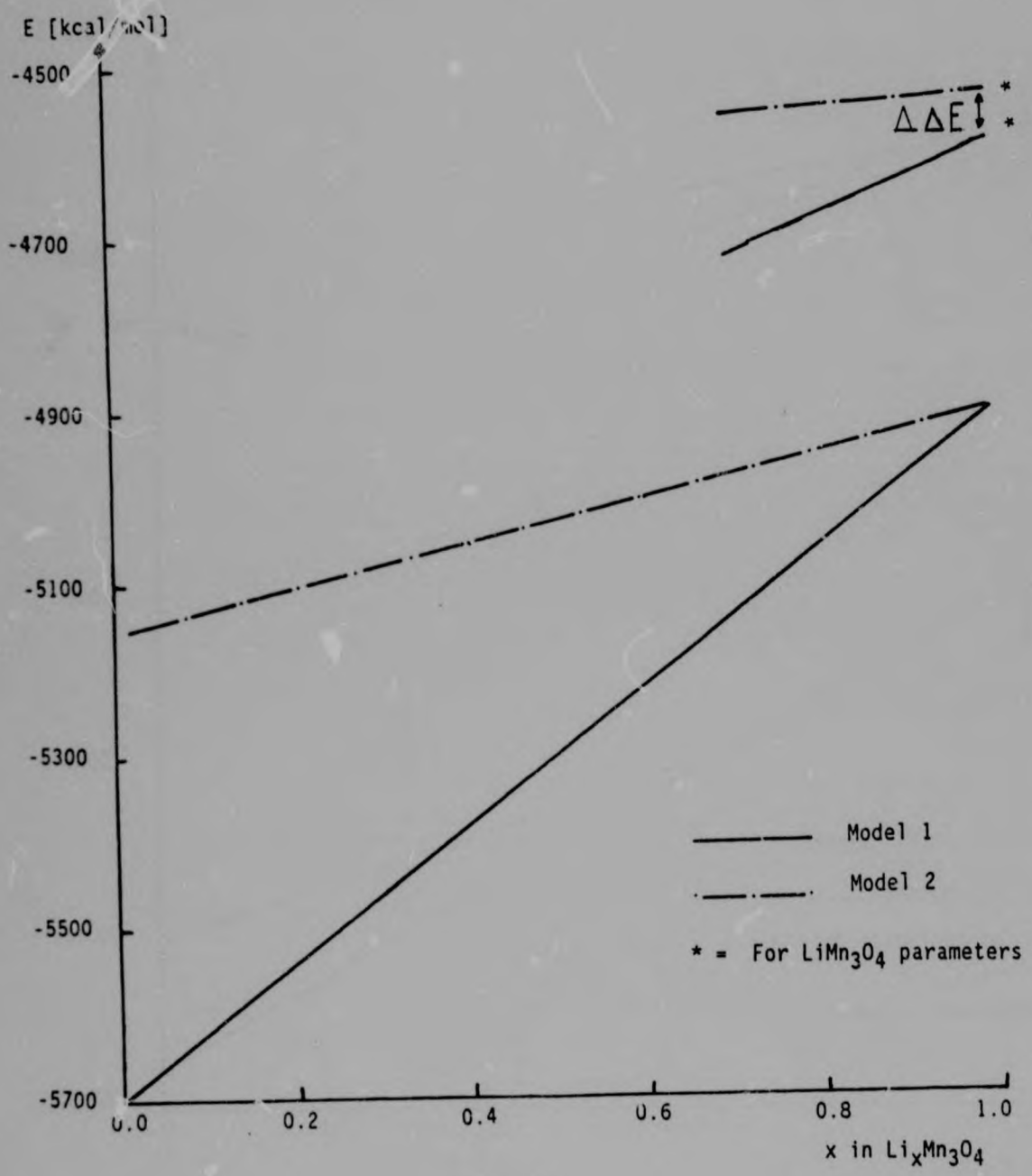

FIG 9.1
Electrostatic energy of $Li_xMn_3O_4$ ($0<x<1$) according to models 1 and 2

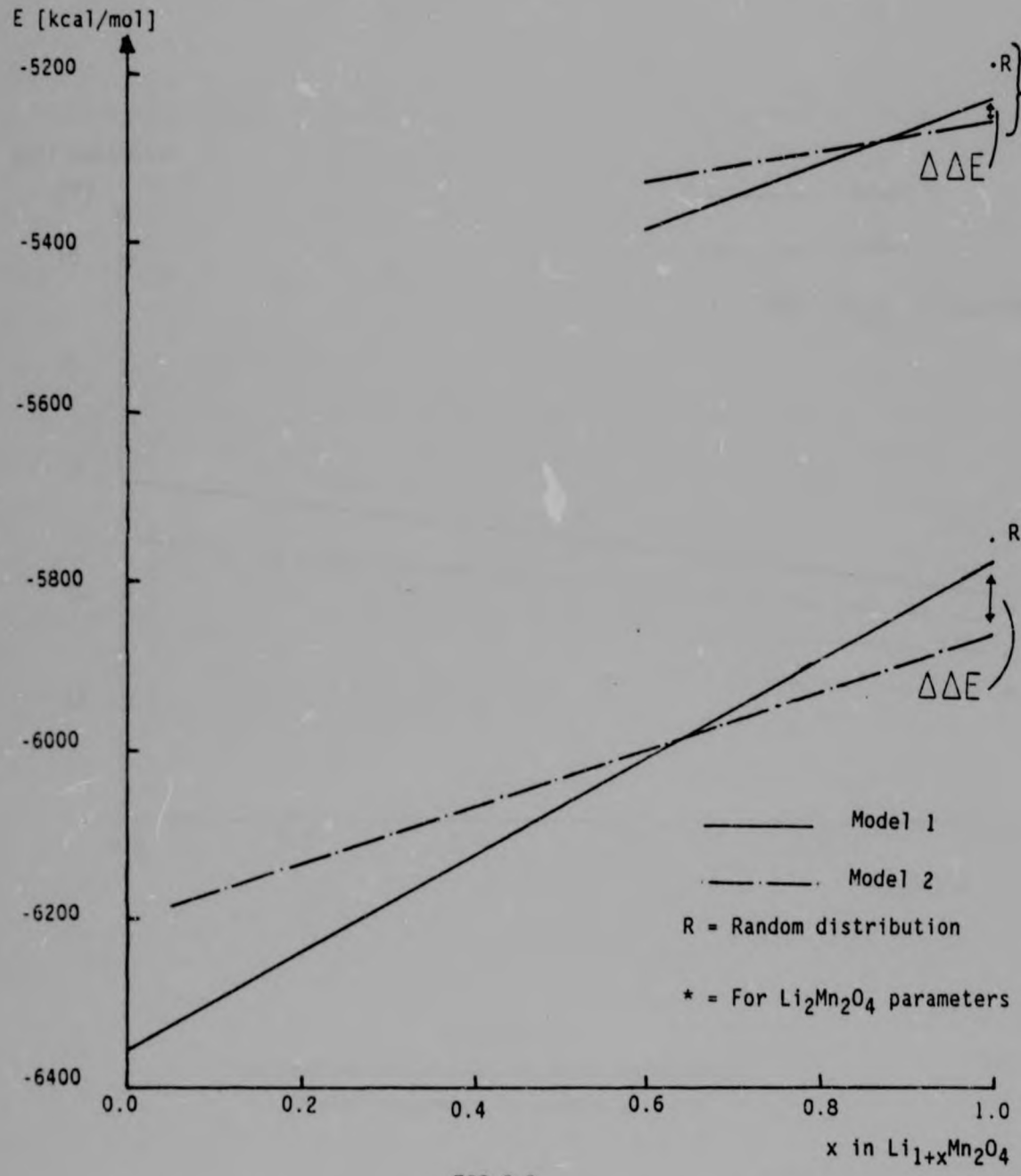

FIG 9.2

Electrostatic energy of $Li_{1+x}Mn_2O_4$ ($0<x<1$) according to models 1, 2 and with a random distribution on the 8a and 16c sites

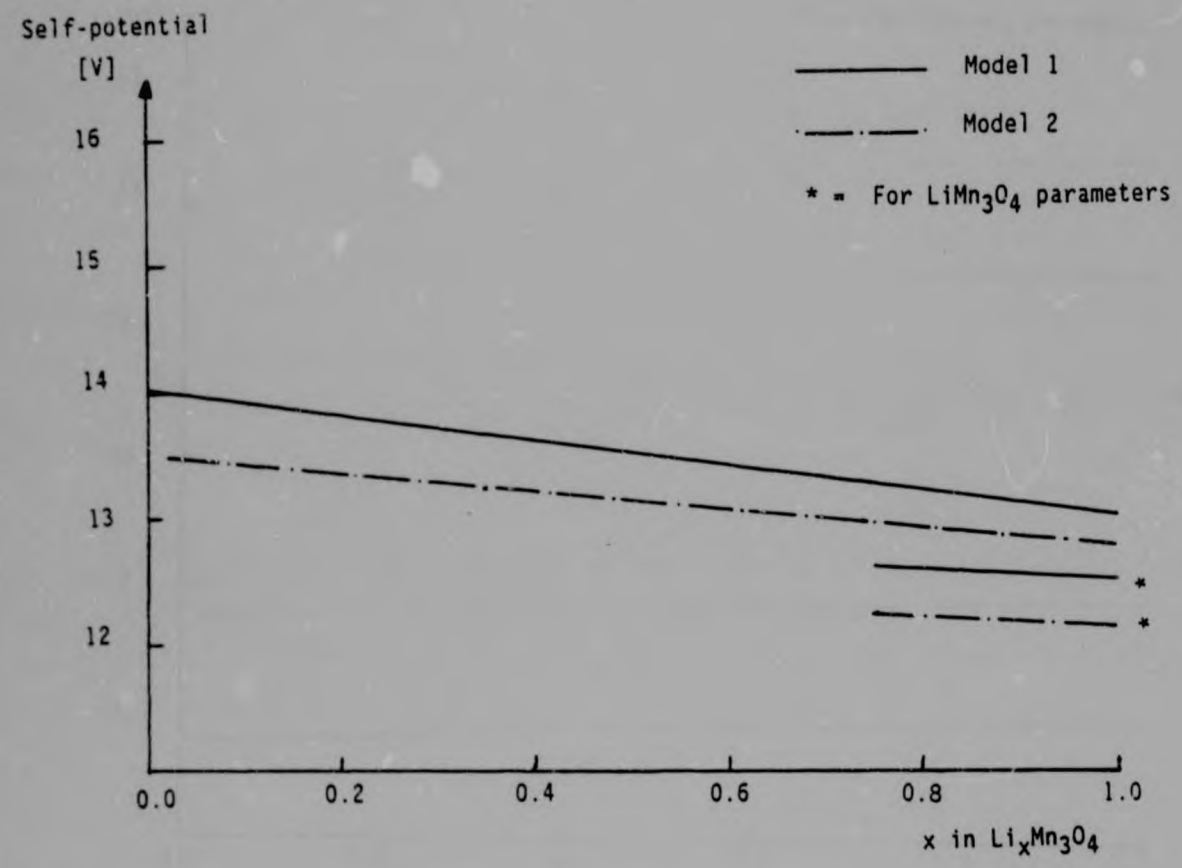

FIG 9.3
Self-potential of the 32e sites in $LixMn_3O_4$
($0<x<1$) according to models 1 and 2

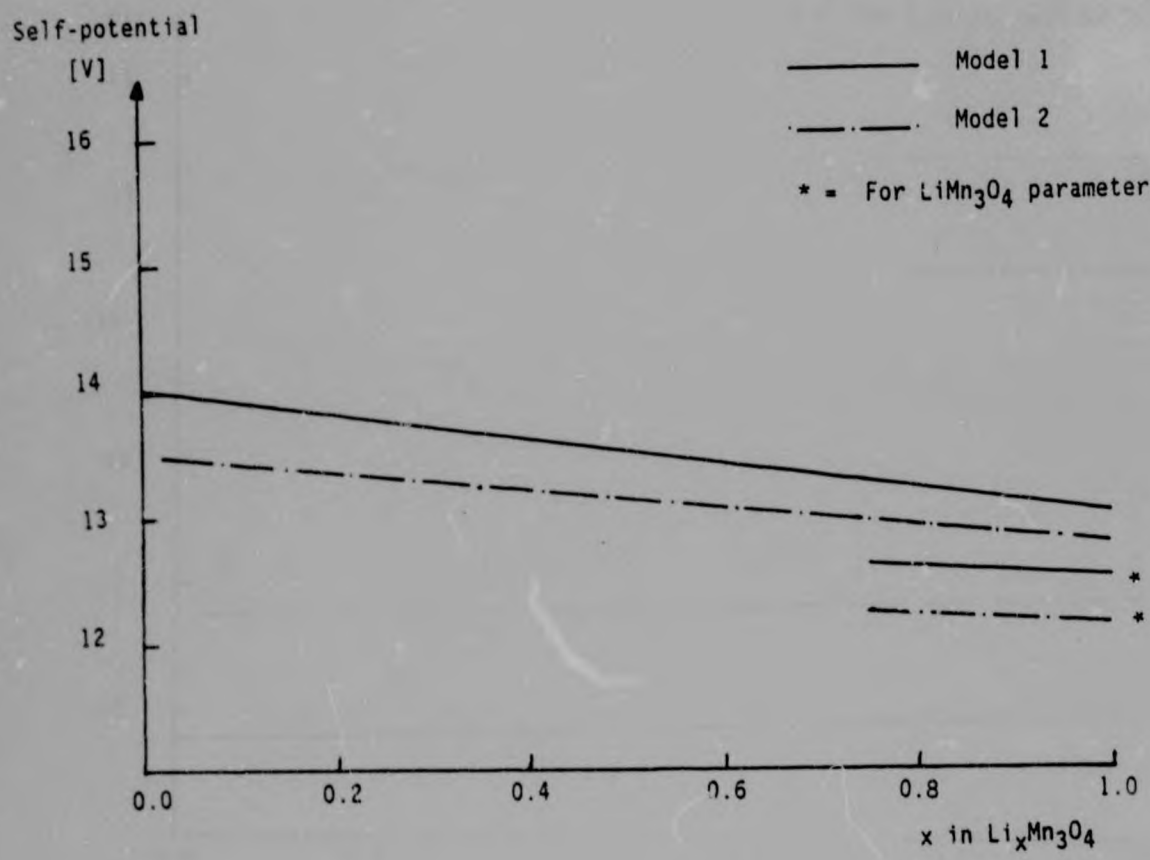

FIG 9.3
Self-potential of the 32e sites in $LixMn_3O_4$
($0<x<1$) according to models 1 and 2

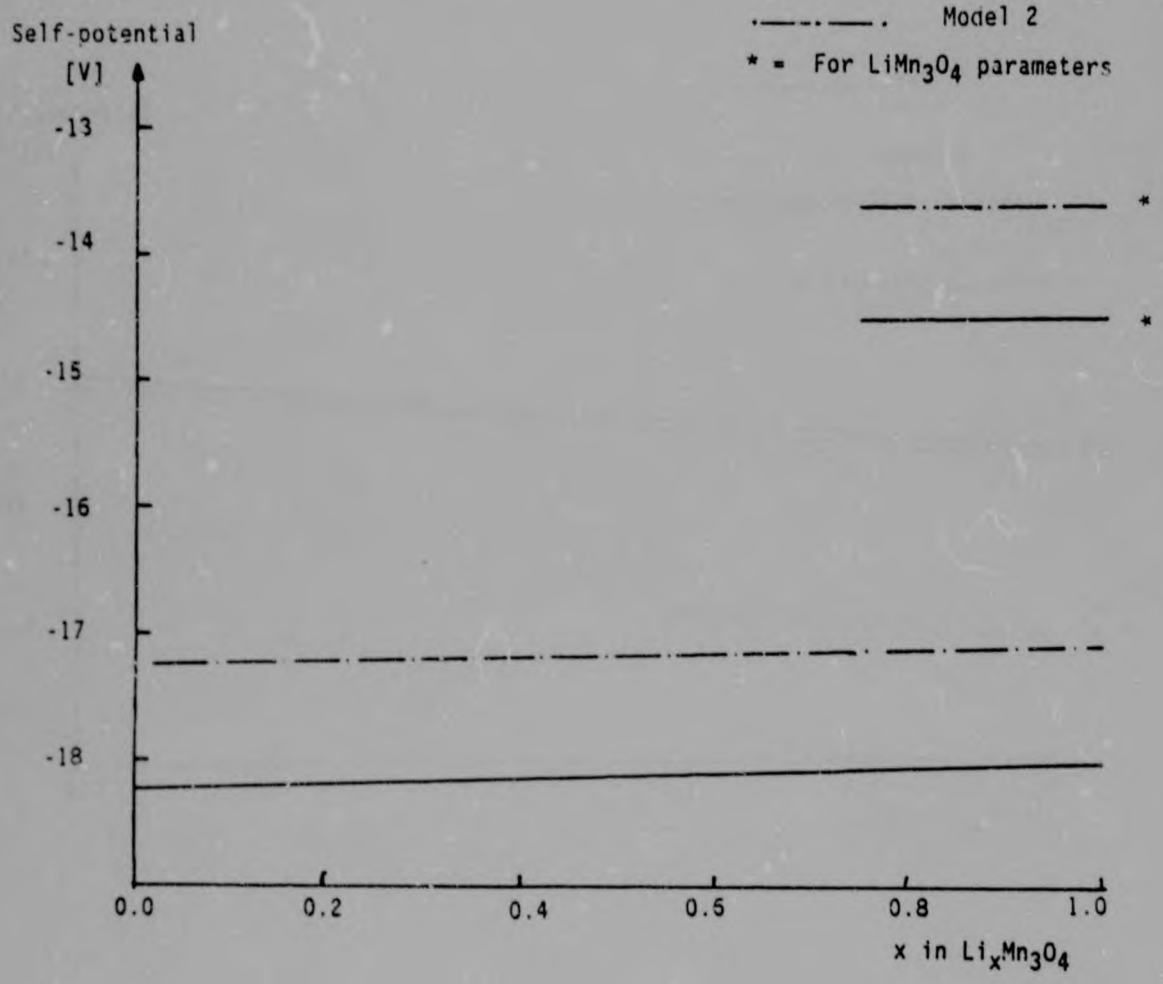

FIG 9.4
Self-potential of the 16d sites in $Li_xMn_3O_4$
($0<x<1$) according to models 1 and 2

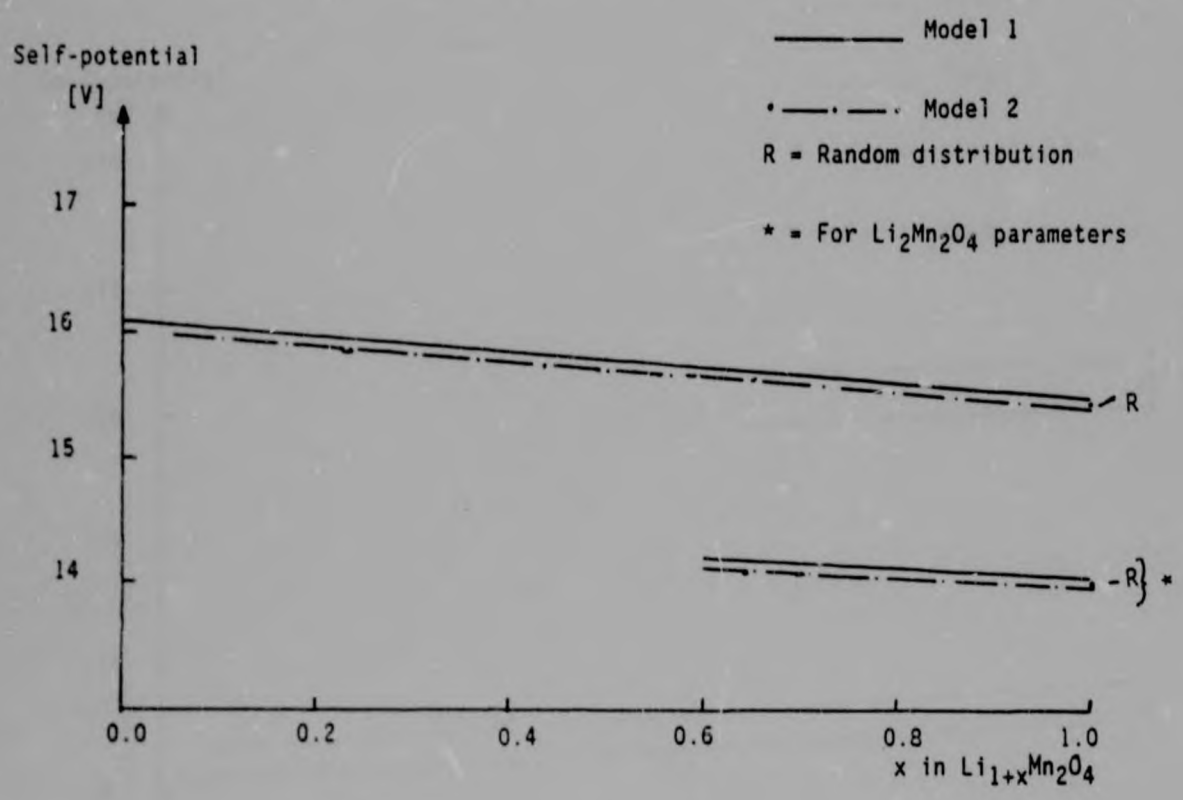

FIG 9.5

Self-potential of the 32e sites in $Li_{1+x}Mn_2O_4$ ($0<x<1$) according to models 1 and 2 and with a random distribution on the 8a and 16c sites

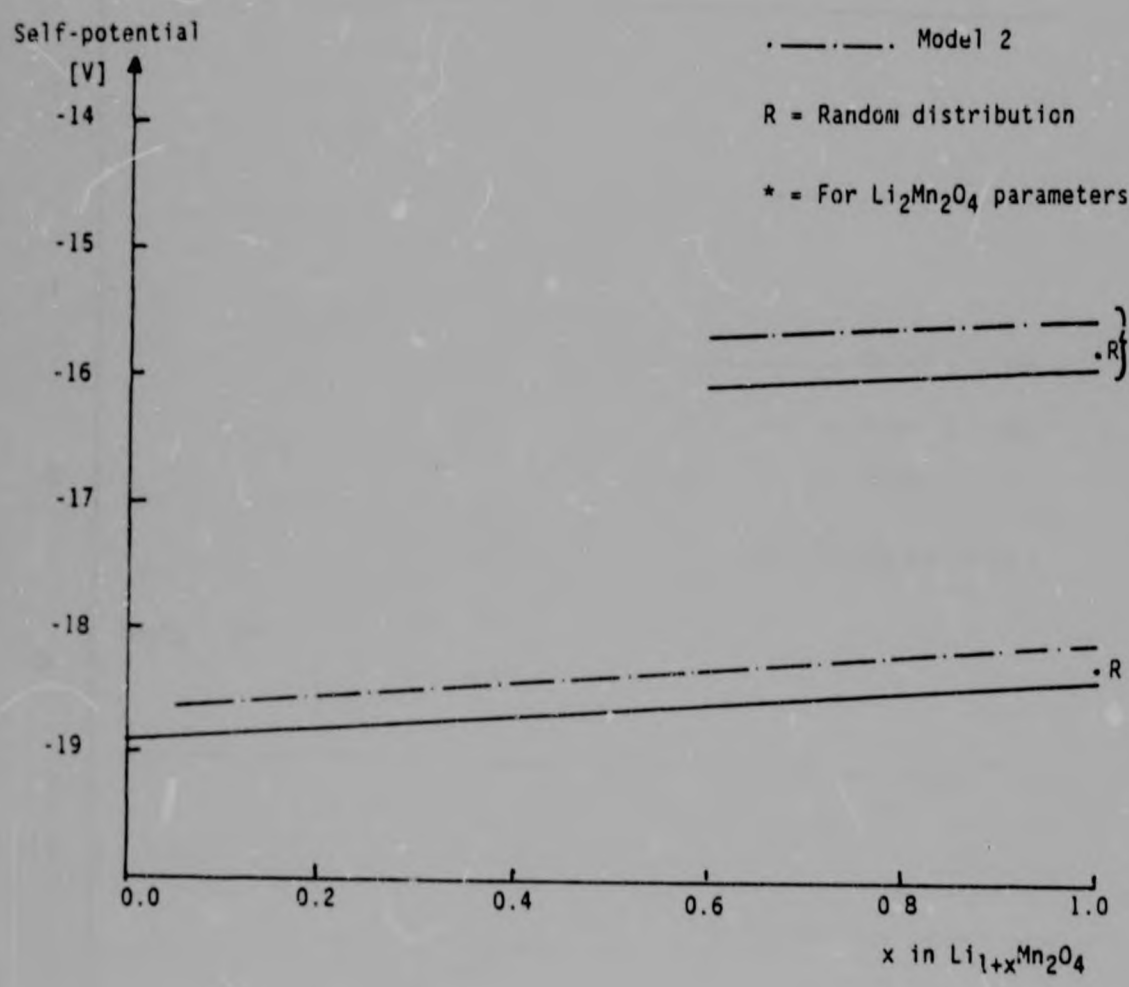

FIG 9.6

Self-potential of the 16d sites in $Li_{1+x}Mn_2O_4$ ($0<x<1$) according to models 1 and 2 and with a random distribution on the 8a and 16c sites

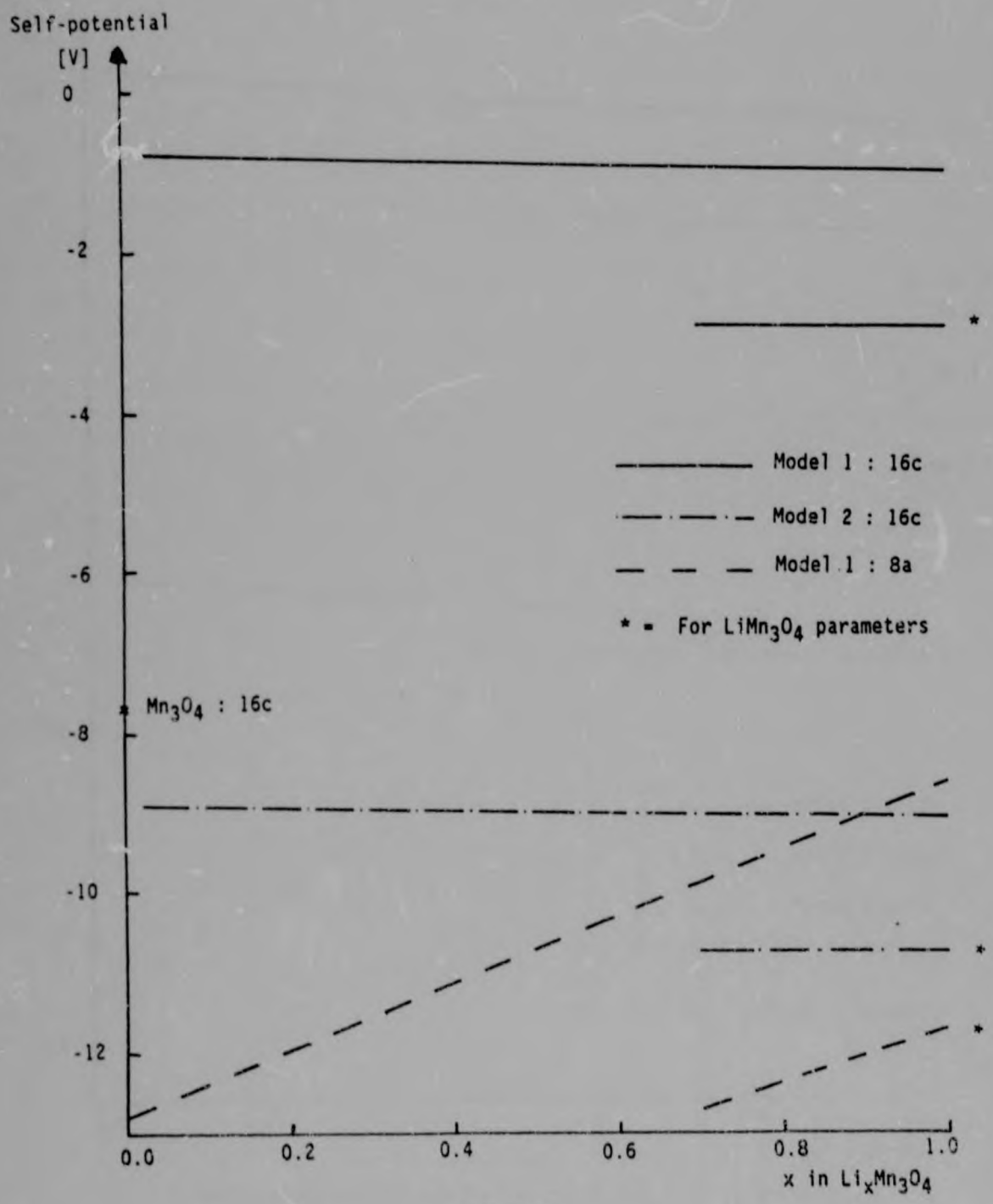

FIG 9.7

Self-potentials of the 8a and 16c sites in $Li_xMn_3O_4$ ($0<x<1$) according to models 1 and 2

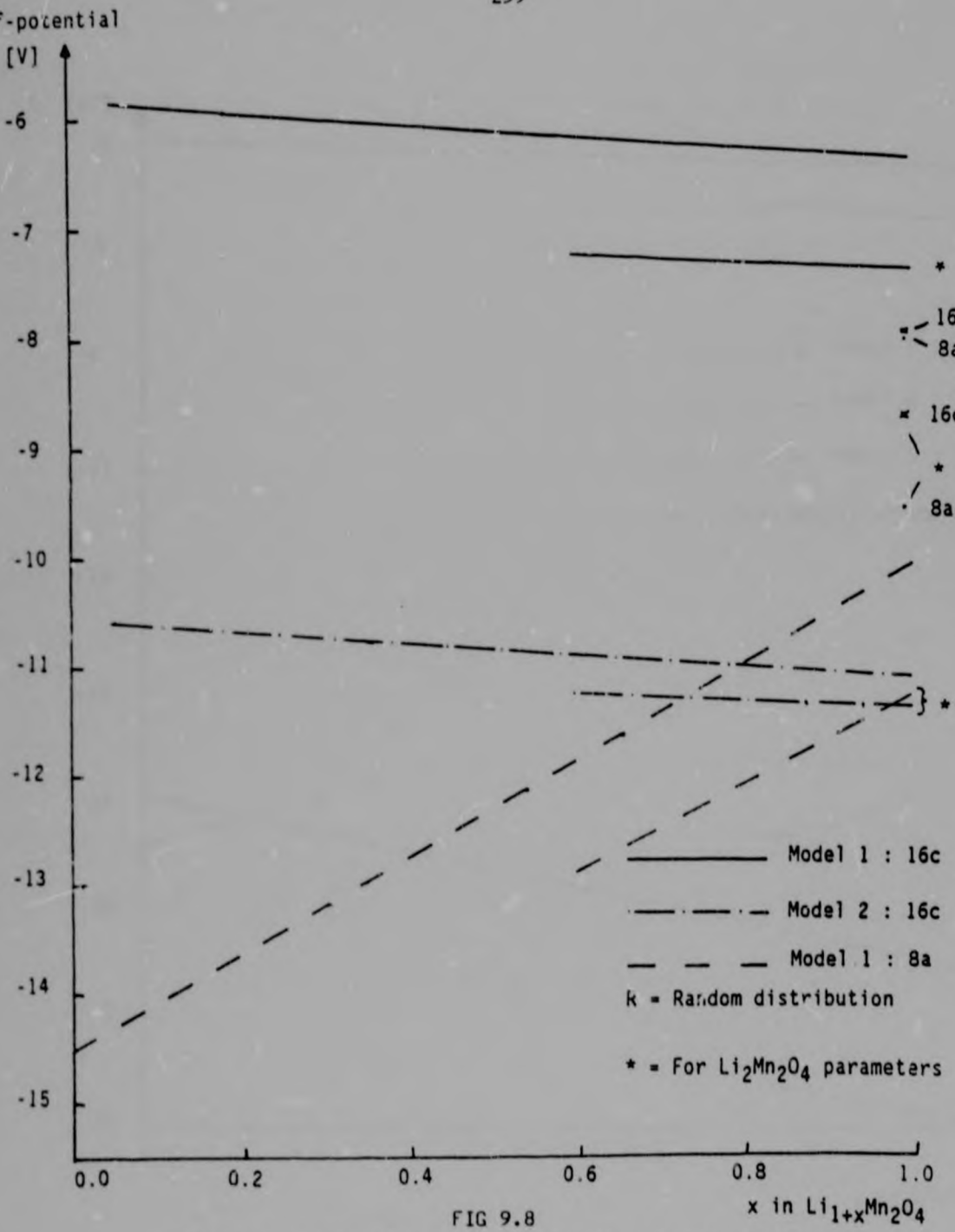

FIG 9.8

Self-potentials of the 8a and 16c sites in $Li_{1+x}Mn_2O_4$ ($0<x<1$) according to models 1 and 2 and with a random distribution on the 8a and 16c sites

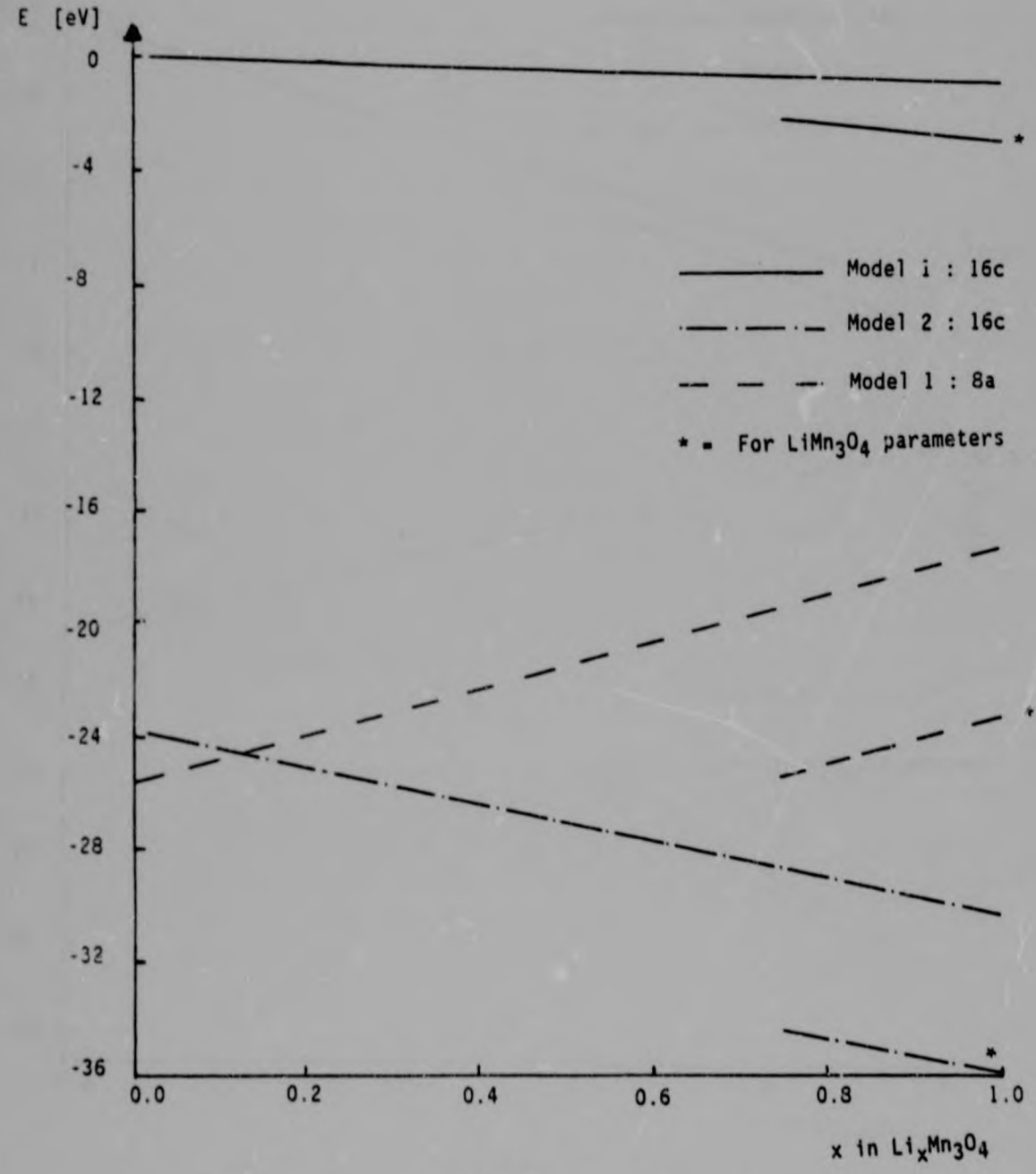

FIG 9.9

Electrostatic energy of the 8a and 16c sites in $Li_xMn_3O_4$ ($0 \leq x \leq 1$) according to models 1 and 2

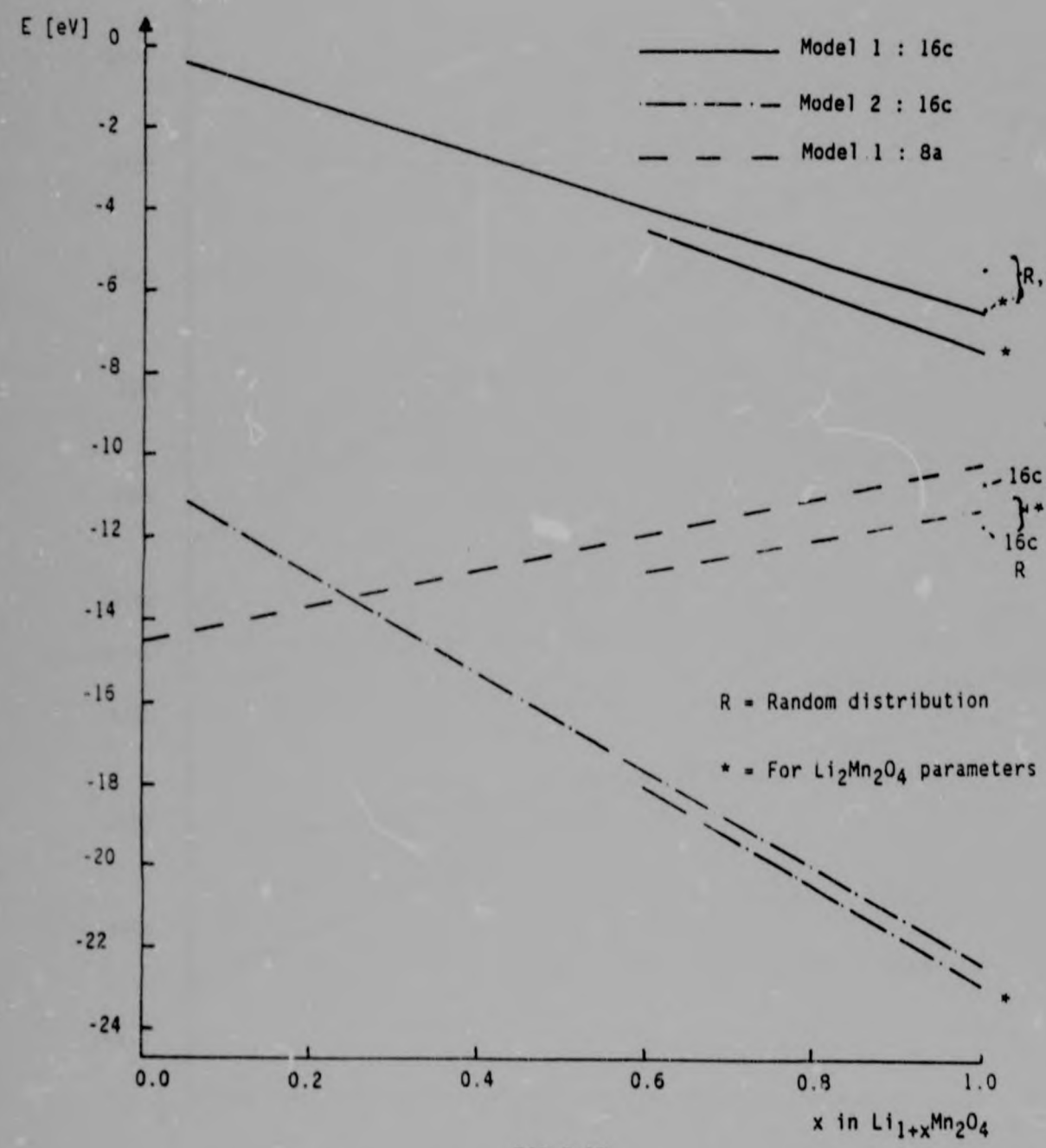

FIG 9.10

Electrostatic energy of the 8a and 16c sites in $Li_{1+x}Mn_2O_4$ ($0 \leq x \leq 1$) according to models 1 and 2 and with a random distribution on the 8a and 16c sites

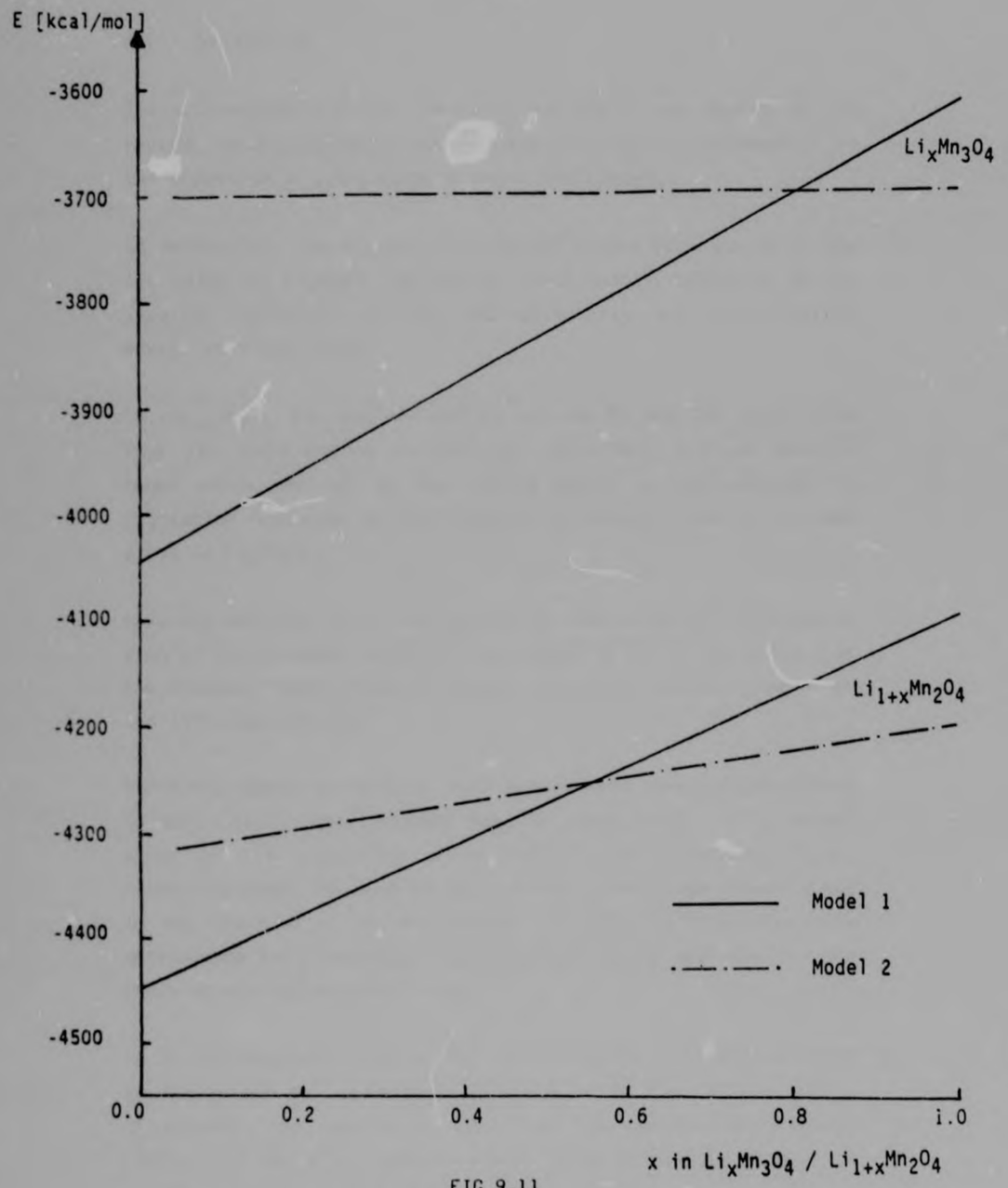

FIG 9.11

Cation-cation interactions in $Li_xMn_3O_4$ and $Li_{1+x}Mn_2O_4$ ($0 \leq x \leq 1$) according to various models

9.11 CONCLUSIONS

The self-potentials and the contributions to the energy of the various crystallographic sites yield some useful information on the mechanism of lithiation of Mn_3O_4 and $LiMn_2O_4$.

In particular, the migration of the Mn^{2+} ions from the 8a to the 16c sites in $Li_xMn_3O_4$ can be at least partly explained by the parallel variation of the self-potentials and electrostatic energy of those sites.

In $Li_{1+x}Mn_2O_4$ the self-potentials of the 8a and 16c sites show that the interactions between the monovalent lithium ions in those sites are not as decisive a factor in determining the lithiation mechanism as the interactions between ions at the same sites in $Li_xMn_3O_4$.

However, although these results are of some value in the explanation of the lithium insertion into spinels, it is now clear that the Madelung energy fails to predict the most stable structure of the lithiated spinels.

Since the energy difference ($\Delta\Delta E$) between the possible structures is very small, other factors must be considered. In a recent study on the prediction of mineral crystal structures [213], Parker stressed the need to include the short-range interactions in the calculation of the lattice energy; in that work, the short-range term comprised the repulsion energy and the van der Waals dipole-dipole interaction.

As it was mentioned earlier (cf section 9.6), the repulsion term is the second most important contribution to the lattice energy of spinels, and amounts to 20-25% of the electrostatic energy [200]; all the other lattice energy terms constitute at most 5% of the coulombic energy.

It has been suggested [200] that the repulsion energy rises as the number of atoms per formula unit increases: whereas the repulsive term amounts to 15 - 18% of the coulombic energy in simple oxides, it is more important in double oxides such as ilmenite (ABO_3) and spinel (AB_2O_4) compounds, where it amounts to as much as 20-25% of the coulombic energy.

According to this observation, the repulsion term of the lithiated spinels would be considerably greater than that of the parent compounds; it is also possible that it influences the relative stability of the various lithiated structures, since it takes into account not only the interionic distances (as in the case of the Madelung energy), but also the radii and the rigidity of the ions. It might thus also allow to differentiate the insertion of, for instance, the various alkali ions.

Another factor which should possibly be taken into account is the energy gain due to ion-relaxation from the centre of site symmetry when an isolated pair share a common face [218].

In conclusion, although the calculation of the self-potentials and energies of the crystallographic sites furthers our understanding of the mechanism of lithium insertion into spinels, it is not sufficient to explain it fully.

The electrostatic energies of the lithiated spinels confirm the metastability of these compounds, but cannot be relied upon to predict the most stable structure. In order to achieve this, other contributions must be taken into account; the calculation of the repulsive energy is suggested as a possible solution.

CHAPTER 10

GENERAL CONCLUSIONS AND SUGGESTIONS FOR FURTHER WORK

The mechanisms and the electrochemistry of the topochemical reactions of lithium with the layered oxide $LiVO_2$ and with the spinel LiV_2O_4 have been studied. From a theoretical point of view, the Madelung energies of the spinel-derived compounds $Li_xMn_3O_4$ and $Li_{1+x}Mn_2O_4$ ($0<x<1$) have been calculated. Since each section of this work comprises an individual detailed discussion of the results, this chapter will be limited to comments of a more general nature.

The usefulness of intercalation reactions in synthetic inorganic chemistry is clearly demonstrated in this work. The topochemical extraction of lithium from $LiVO_2$ is used in a new route developed for the synthesis of the normal spinel $Li[V_2]O_4$. This compound is accessible using more conventional, high temperature techniques, but it is generally contaminated with other vanadium oxides.

Intercalation reactions also allow the preparation of metastable compounds with unusual structures, which cannot be obtained by other methods. Examples in this work are the lithium-deficient spinel $Li_{0.9}V_2O_4$ and the partially ordered rocksalt phase $\{Li_2\}_{16c}[V_2]_{16d}O_4$. The latter can be considered a new polymorph of $LiVO_2$: α-$LiVO_2$ has a layered structure. Another cubic phase of $LiVO_2$ has previously been prepared at high pressure [214]. The structure of this phase was described as $\{Li_{1/3}V_{2/3}\}_{16c}[Li_{2/3}V_{1/3}]_{16d}O_4$, using the Fd3m space-group.

A more technical application of intercalation reactions in reversible electrochemical systems is shown in chapters 6 and 7 where the system $Li_{1\pm x}V_2O_4$ ($0<x<1$) is examined.

Early studies on lithium intercalation into transition metal oxides and sulphides relied largely upon structural considerations for the selection of potential electrode materials for lithium batteries. It is now widely ackrowledged that, although structural characteristics play an important role, other factors may significantly impair electrochemical performance.

The coordination and the oxidation state can affect the radius, the relative stability and the mobility of a transition metal cation. As the oxidation state of the latter changes in the course of the topochemical reaction, the isostructural compounds may be stabilised or destabilised to different extents. Electrochemical oxidation/reduction potentials vary widely when comparing transition metals; other factors, which play a role in the reaction kinetics and mechanism, e.g. electronic conductivity, may differ within a group of isostructural compounds.

In this work, the structural and electrochemical characteristics of products derived from $LiVO_2$ and LiV_2O_4 were discussed and compared with compounds obtained from the isostructural materials $LiMO_2$ (M = Co, Ni) and LiM_2O_4 (M = Ti, Mn) respectively. Although a few general patterns do emerge, a number of differences significantly alter the electrochemical properties, as discussed in the concluding sections of chapters 4, 6 and 7.

An important feature in the vanadium compounds examined here is the mobility of the vanadium cation. It is evidenced in both $LiVO_2$ and LiV_2O_4 by the high isotropic temperature factors of the vanadium cation in many of the derivatives and by the ion migration within the lattice, observed in the course of the delithiation reactions. This structural rearrangement is irreversible; as a result, delithiation is irreversible.

By contrast, the cobalt and manganese cations are less mobile and no significant structural modification occurs in either $Li_{1-x}CoO_2$ or $Li_{1-x}Mn_2O_4$ ($0<x\leq1$); these compounds can therefore be reversibly relithiated.

Lithium-ion diffusion rates in intercalation compounds are often related to the structures of the host lattice. In this work, Li^+ diffusion rates were measured on polycrystalline samples of various lithium vanadium oxides; although absolute diffusion rates cannot be obtained by this method (cf section 2.6.3), the relative values can be compared with a fair degree of confidence.

Results presented here indicate that the Li^+ diffusion rate is highest in $Li_2V_2O_4$ (ordered rocksalt structure), intermediate in $LiVO_2$ (layered structure) and lowest in LiV_2O_4 (spinel structure). Although this suggests that three-dimensional networks allow faster Li^+-ion diffusion than the two-dimensional layered systems, it must be stressed that only single crystal measurements could provide conclusive evidence to this effect. It has in fact been shown that the electrochemical behaviour of a polycrystalline electrode can often be correlated to a diffusion-space dimension which depends on geometric factors, rather than on the crystal structure [114]. However, it must be stressed that, although results obtained with single crystals are more accurate, they are of interest from a more theoretical point of view, since they do not reflect the behaviour of the material in a practical lithium cell, where the electrode is generally polycrystalline.

The results presented here suggest that the spinel LiV_2O_4 is a promising candidate as an electrode for a secondary lithium battery.

In a comparative study on vanadium oxides as electrode materials for rechargeable lithium cells, West et al. suggest that an open structure and a fairly low density are important considerations when selecting electrode materials which operate via a topochemical process [84]. The density of LiV_2O_4 (ρ = 4.1 g cm^{-3}) is only slightly higher than that of the extremely promising vanadium oxide V_6O_{13} (ρ = 3.9 g cm^{-3}); it is lower than the rutile phase VO_2 (ρ = 4.6 g cm^{-3}) into which only a limited amount of lithium can be inserted [25].

Lithium insertion into LiV_2O_4 is reversible and exhibits a relatively high operating voltage of ~2.35 V. The theoretical energy density for the system $Li_{1+x}V_2O_4$ ($0 \leq x \leq 1$) amounts to ~350 Wh kg^{-1}. This value is lower than that of a number of the more promising vanadium oxides (e.g. V_6O_{13}, V_2O_5 and $Li_{1\pm x}V_3O_8$). However, in practice, the energy density of a number of these electrodes is reduced, since many of them cannot be cycled over the entire compositional range.

The cyclic voltammetry results presented here and preliminary cell cycling tests [215 - 217] indicate that, at ambient temperature, it is possible to cycle reversibly at least one Li^+ per $[V_2]O_4$ unit. This electrode capacity is only slightly inferior to that of V_6O_{13} (3.6 Li/V_6O_{13} at 150 °C) and $Li_{1+x}V_3O_8$ (2 Li/V_3O_8 at ambient temperature) [84].

In addition, the lithium diffusion rates measured in the system $Li_{1+x}V_2O_4$ ($0 \leq x \leq 1$), which vary between 4.10^{-10} cm^2 sec^{-1} $< \tilde{D} <$ 6.10^{-8} cm^2 sec^{-1}, are sufficiently high to allow acceptable current density levels in practical lithium cells.

These promising properties have prompted cell cycling tests, preliminary results of which have been published recently [215,216]. It has also been suggested that the electrode capacity is greater than anticipated and that it is possible to cycle at least 2 Li^+ in and out of $Li_{1+x}V_2O_4$ [217]. The operating mechanism of an electrode $Li_{1+x}V_2O_4$, where $x > 1$, is still unknown: structural studies would provide an answer to this question.

Lithium extraction from LiV_2O_4 beyond $x \approx 0.3$ in $Li_{1-x}V_2O_4$ was shown here to be irreversible. A reversible delithiation of the spinel would obviously be an advantage, since it would extend the electrode capacity.

In this work, a fraction of Li^+ cations was substituted with Zn^{2+} cations, in order to stabilise the $[V_2]O_4$ sub-lattice in

$Li_{1-x}V_2O_4$ ($x > 0.4$). This attempt was met with limited success, since, for low lithium content, zinc cations were extracted concurrently from the spinel structure.

An alternative approach could be the introduction of a fraction of transition metal cations on the tetrahedral sites, leading to a composition $Li_{1-y}M_y[V_2]O_4$. The transition metal cations would not be extracted as readily as the Li^+ or Zn^{2+} cations, since they are more strongly bonded. They would possibly provide sufficient electrostatic interaction between oxide layers in the delithiated product to maintain the $[V_2]O_4$ sub-lattice intact. Vanadium or molybdenum are suggested as possible dopants.

APPENDIX

CONTRIBUTION OF VARIOUS ATOM POSITIONS TO THE INTENSITIES OF SELECTED REFLECTIONS IN THE $Fd\bar{3}m$ AND $R\bar{3}m$ SPACE GROUPS

Throughout this work, the migration of atoms within the lattice during insertion/extraction reactions is discussed. It is largely detected by the variation of the relative intensities of a few key reflections in the powder X-ray diffraction patterns.

The contribution of atoms located in specific sites to the intensity of a particular reflection is contained in the phase term (ϕ) of the structure factor (F_{hkl}):

$$F_{hkl} = A.e^{i\phi} \qquad (A.1)$$

where A = amplitude
ϕ = phase

$$\text{with } \phi = 2\pi (hu + kv + lw) \qquad (2.2)$$

where hkl = Miller indices
uvw = fractional coordinates.

The complete expression of the structure factor is recalled here (c.f. section 2.1.4.2):

$$F_{hkl} = \sum_{n=1}^{N} f_n \, e^{2\pi i (hu_n + kv_n + lw_n)} \qquad (2.11)$$

where f_n = scattering factor of the atom n
hkl = as above
uvw = as above.

The intensity of a reflection is proportional to $|F_{hkl}|^2$, which can be expressed as:

$$|F_{hkl}|^2 = A_{hkl}^2 + B_{hkl}^2 \qquad (A.2)$$

where A_{hkl} and B_{hkl} are projections of F_{hkl} on the x and y axes, and are given by the equations:

$$A_{hkl} = \sum_n f_n \cos 2\pi (hu_n + kv_n + lw_n) \qquad (A.3)$$

$$B_{hkl} = \sum_n f_n \sin 2\pi (hu_n + kv_n + lw_n) \qquad (A.4)$$

The contribution of the various atom positions to a particular reflection can therefore be calculated, using equations A.3 and A.4.

The contribution of atom positions to the intensity of a few reflections in the cubic spinel space group $Fd\bar{3}m$ and in the trigonal ($LiMO_2$ compounds) $R\bar{3}m$ space group are given here in the form of the expressions:

$$a = \cos 2\pi (hu_n + kv_n + lw_n) \qquad (A.5)$$

$$b = \sin 2\pi (hu_n + kv_n + lw_n) \qquad (A.6)$$

$|F_{hkl}|^2$ can then be obtained from A.7:

$$|F_{hkl}|^2 = (\sum_n f_n a)^2 + (\sum_n f_n b)^2 \qquad (A.7)$$

where f_n = scattering factor of the atom n
hkl = as above
uvw = as above.

The intensity of a reflection is proportional to $|F_{hkl}|^2$, which can be expressed as:

$$|F_{hkl}|^2 = A^2_{hkl} + B^2_{hkl} \qquad (A.2)$$

where A_{hkl} and B_{hkl} are projections of F_{hkl} on the x and y axes, and are given by the equations:

$$A_{hkl} = \sum_n f_n \cos 2\pi (hu_n + kv_n + lw_n) \qquad (A.3)$$

$$B_{hkl} = \sum_n f_n \sin 2\pi (hu_n + kv_n + lw_n) \qquad (A.4)$$

The contribution of the various atom positions to a particular reflection can therefore be calculated, using equations A.3 and A.4.

The contribution of atom positions to the intensity of a few reflections in the cubic spinel space group Fd3m and in the trigonal ($LiMO_2$ compounds) $R\bar{3}m$ space group are given here in the form of the expressions:

$$a = \cos 2\pi (hu_n + kv_n + lw_n) \qquad (A.5)$$

$$b = \sin 2\pi (hu_n + kv_n + lw_n) \qquad (A.6)$$

$|F_{hkl}|^2$ can then be obtained from A.7:

$$|F_{hkl}|^2 = (\sum_n f_n a)^2 + (\sum_n f_n b)^2 \qquad (A.7)$$

A.1 SPACE GROUP: Fd3m

TABLE A.1

Atom positions for the space group Fd3m

Site	u	v	w
8a	0.125	0.125	0.125
16c	0.000	0.000	0.000
16d	0.500	0.500	0.500
32e*	0.250	0.250	0.250

* The position 32e describes the anion site in spinels. An ideal value of u = 0.250 is used here for simplicity.

TABLE A.2

Values of a, b in the space group Fd3m for a few reflections

hkl	Site	hu + kv + lw	a	b
111	8a	0.375	-0.707	0.707
	16c	0	1	0
	16d	1.5	-1	0
	32e	0.75	0	-1
311	8a	0.625	-0.707	-0.707
	16c	0	1	0
	16d	2.5	-1	0
	32e	1.25	0	1
222	8a	0.75	0	-1
	16c	0	1	0
	16d	3	1	0
	32e	1.5	-1	0
400	8a	0.5	-1	0
	16c	0	1	0
	16d	2.0	1	0
	32e	1.0	1	0

TABLE A.2 (Cont.)

Values of a, b in the space group Fd3m for a few reflections

hkl	Site	hu + kv + lw	a	b
440	8a	1.0	1	0
	16c	0	1	0
	16d	4.0	1	0
	32e	2.0	1	0
444	8a	1.5	-1	0
	16c	0	1	0
	16d	6.0	1	0
	32e	3.0	1	0

It is to be noted that atoms in the 8a, 16c, 16d and 32e sites all scatter in phase in the case of the {440} reflection.

A.2 SPACE GROUP : $R\bar{3}m$

TABLE A.3

Atom positions for the space group $R\bar{3}m$

Site	u	v	w
3a	0	0	0
3b	0	0	0.5
6c* (O^{2-})	0	0	0.25
6c** (T1)	0	0	0.125
6c** (T2)	0	0	0.375

* Anion position in $LiMO_2$ (M = V, Co, Cr, Ni) structure

** Vacant tetrahedral sites in $LiMO_2$ structure

TABLE A.4

Values of a, b in the space group $R\bar{3}m$ for a few reflections

hkl	Site	hu + kv + lw	a	b
003	3a	0	1	0
	3b	1.5	-1	0
	6c (O^{-2})	0.75	0	-1
	6c (T1)	0.375	-0.707	0.707
	6c (T2)	1.125	0.707	0.707
006	3a	0	1	0
	3b	3	1	0
	6c (O^{-2})	1.5	-1	0
	6c (T1)	0.75	0	-1
	6c (T2)	2.25	0	+1
101	3a	0	+1	0
	3b	0.5	-1	0
	6c (O^{-2})	0.25	0	+1
	6c (T1)	0.125	+0.707	+0.707
	6c (T2)	0.375	-0.707	+0.707
012	3a	0	1	0
	3b	1	1	0
	6c (O^{-2})	0.5	-1	0
	6c (T1)	0.25	0	+1
	6c (T2)	0.75	0	-1
104	3a	0	1	0
	3b	2.0	1	0
	6c (O^{-2})	1.0	1	0
	6c (T1)	0.5	-1	0
	6c (T2)	1.5	-1	0
018	3a	0	1	0
	3b	4	1	0
	6c (O^{-2})	2	1	0
	6c (T1)	1	1	0
	6c (T2)	3	1	0

TABLE A.4 (Cont.)

Values of a, b in the space group $R\bar{3}m$ for a few reflections

hkl	Site	hu + kv + lw	a	b
110	3a	0	1	0
	3b	0	1	0
	6c (0^{-2})	0	1	0
	6c (T1)	0	1	0
	6c (T2)	0	1	0

It is to be noted that atoms in 3a, 3b and 6c sites all scatter in phase in the case of the {018} and {110} reflections.

REFERENCES

[1] M Ewing, Electron. Power, **28,** 523 (1982)

[2] J C Posa, Electronic Design, March 14, (1985), p 43

[3] J -I Yamaki, J. Power Sources **20,** 3 (1987)

[4] R Schöllhorn, Angew. Chem. **92,** 1015 (1980)

[5] R Schöllhorn, Physica **99B,** 89 (1980)

[6] R F Grim, Clay Mineralogy, Mc Graw Hill, New York (1968)

[7] F F Chang, B L Gilbert and T I Sun, J. Electrochem. Soc. **122,** 955 (1975)

[8] B Reichman and A J Bard, J. Electrochem. Soc. **126,** 2133 (1979)

[9] D W Murphy and P A Christian, Science, **205,** 651 (1979)

[10] M S Whittingham, Progress in Solid State Chem. **12,** 41 (1978)

[11] K M Abraham, Solid State Ionics **7,** 199 (1982)

[12] D W Murphy and J A Trumbore, J. Cryst. Growth **39,** 185 (1977)

[13] M S Whittingham, J. Electrochem. Soc. **123,** 315 (1976)

[14] W Rüdorff and H H Sick, Angew. Chem. **71,** 127 (1959)

[15] M S Whittingham, Science **192,** 1126 (1976)

[16] G Pistoia, J. Power Sources **9,** 307 (1983)

[17] J O Besenhard and R Schöllhorn, J. Power Sources **1,** 267 (1976)

[18] M Pasquali, G Pistoia and F Rodante, Solid State Ionics **6,** 319 (1982)

[19] J O Besenhard, J Heydecke and H P Fritz, Solid State Ionics **6,** 215 (1982)

[20] K Mizushima, P C Jones, P J Wiseman and J B Goodenough, Mater. Res. Bull. **15,** 783 (1980)

[21] D W Murphy, P A Christian, F J Di Salvo, J N Carides and J V Waszczak, J. Electrochem. Soc. **128,** 2053 (1981)

[22] D W Murphy, P A Christian, F J Di Salvo and J V Waszczak, Inorg. Chem. **18,** 2800 (1979)

[23] A Le Méhauté, J. Power Sources **9,** 167 (1983)

[24] J O Besenhard and R Schöllhorn, J. Electrochem. Soc. **124,** 968 (1977)

[25] D W Murphy, F J Di Salvo, J N Carides and J V Waszczak, Mater. Res. Bull. **13,** 1395 (1978)

[26] M Eisenberg, J. Electrochem. Soc. **127,** 2382 (1980)

[27] M M Thackeray and J Coetzer, Mater. Res. Bull. **16,** 591 (1981)

[28] M M Thackeray, W I F David and J B Goodenough, Mater. Res. Bull. **17,** 785 (1982)

[29] I D Raistrick, N A Godshall and R A Huggins, U S Patent 4, 340, 652 (1982)

[30] N A Godshall, I D Raistrick and R A Huggins, J. Electrochem. Soc. **131,** 543 (1984)

[31] L A de Picciotto and M M Thackeray, Mater. Res. Bull. **21,** 583 (1986)

[32] C J Chen, M Greenblatt and J V Waszczak, J. Solid State Chem. **64,** 240 (1986)

[33] M M Thackeray, W I F David, P G Bruce and J B Goodenough, Mater. Res. Bull. **18,** 461 (1983)

[34] M M Thackeray, S D Baker, K T Adendorff and J B Goodenough, Solid State Ionics **17,** 175 (1985)

[35] R J Bouchard, P A Russo and A Wold, Inorg. Chem. **4,** 685 (1965)

[36] W H Bragg, Nature **95,** 561 (1915)

[37] T F W Barth and E Posnjak, Z. Kristallogr. **82,** 325 (1932)

[38] G Blasse, Philips Res. Rep. Suppl. 3 (1964)

[39] E W Gorter, Philips Res. Rep. **9,** 295 (1954)

[40] R J Hill, J R Craig and G V Gibbs, Phys. and Chem. Miner. **4,** 317 (1979)

[41] L Pauling, The Nature of the chemical bond, 3rd ed., Cornell University Press, New York (1960)

[42] M Iizumi and G Shirane, Solid State Commun. **17,** 433 (1975)

[43] J Yoshida and S Iida, J. Phys. Soc. Japan **42,** 230 (1977)

[44] G W van Oosterhout and C J M Rooijmans, Nature **181,** 44 (1958)

[45] C Greaves, J. Solid State Chem. **49,** 325 (1983)

[24] J O Besenhard and R Schöllhorn, J. Electrochem. Soc. **124,** 968 (1977)

[25] D W Murphy, F J Di Salvo, J N Carides and J V Waszczak, Mater. Res. Bull. **13,** 1395 (1978)

[26] M Eisenberg, J. Electrochem. Soc. **127,** 2382 (1980)

[27] M M Thackeray and J Coetzer, Mater. Res. Bull. **16,** 591 (1981)

[28] M M Thackeray, W I F David and J B Goodenough, Mater. Res. Bull. **17,** 785 (1982)

[29] I D Raistrick, N A Godshall and R A Huggins, U S Patent 4, 340, 652 (1982)

[30] N A Godshall, I D Raistrick and R A Huggins, J. Electrochem. Soc. **131,** 543 (1984)

[31] L A de Picciotto and M M Thackeray, Mater. Res. Bull. **21,** 583 (1986)

[32] C J Chen, M Greenblatt and J V Waszczak, J. Solid State Chem. **64,** 240 (1986)

[33] M M Thackeray, W I F David, P G Bruce and J B Goodenough, Mater. Res. Bull. **18,** 461 (1983)

[34] M M Thackeray, S D Baker, K T Adendorff and J B Goodenough, Solid State Ionics **17,** 175 (1985)

[35] R J Bouchard, P A Russo and A Wold, Inorg. Chem. **4,** 685 (1965)

[36] W H Bragg, Nature **95,** 561 (1915)

[37] T F W Barth and E Posnjak, Z. Kristallogr. **82,** 325 (1932)

[38] G Blasse, Philips Res. Rep. Suppl. 3 (1964)

[39] E W Gorter, Philips Res. Rep. **9,** 295 (1954)

[40] R J Hill, J R Craig and G V Gibbs, Phys. and Chem. Miner. **4,** 317 (1979)

[41] L Pauling, The Nature of the chemical bond, 3rd ed., Cornell University Press, New York (1960)

[42] M Iizumi and G Shirane, Solid State Commun. **17,** 433 (1975)

[43] J Yoshida and S Iida, J. Phys. Soc. Japan **42,** 230 (1977)

[44] G W van Oosterhout and C J M Rooijmans, Nature **181,** 44 (1958)

[45] C Greaves, J. Solid State Chem. **49,** 325 (1983)

[46] J C Joubert and A Durif, Bull. Soc. Chim. Fr. Mineral. Cristallogr. **89,** 26 (1966)

[47] G H Stauss, J. Chem. Phys. **40,** 1988 (1964)

[48] J B Goodenough and A L Loeb, Phys. Rev. **98,** 391 (1955)

[49] J D Dunitz and L E Orgel, J. Phys. Chem. Solids **3,** 20 (1957)

[50] R Buhl, J. Phys. Chem. Solids **30,** 805 (1969)

[51] H Ohnishi and T Teranashi, J. Phys. Soc. Japan **16,** 35 (1961)

[52] C D Spencer, P A Smith and R P Stillwell, J. Phys. Chem. Solids **39,** 103 (1978)

[53] E F Bertaut, Compt. Rend. **230,** 213 (1950); Errata, ibidem, **231,** 88 (1951)

[54] H Fuhurashi, M Inagaki and S Naka, J. Inorg. Nucl. Chem. **35,** 3009 (1973)

[55] L Gastaldi and A Lapiccirella, J. Solid State Chem. **30,** 223 (1979)

[56] E J W Verwey and E L Heilmann, J. Chem. Phys. **15,** 174 (1947)

[57] E J W Verwey, F de Boer and J H van Santen, J. Chem. Phys. **16,** 1091 (1948)

[58] D S McClure, J. Phys. Chem. Solids **3,** 311 (1957)

[59] J D Dunitz and L E Orgel, J. Phys. Chem. Solids **3,** 318 (1957)

[60] F A Cotton, J. Chem. Educ. **41,** 466 (1964)

[61] L Hermans, J Weenk and W van Gool, Z. für Phys. Chem. **88,** 15 (1974)

[62] P Thompson and N W Grimes, Philos. Mag. **36,** 501 (1977)

[63] C Glidewell, Inorg. Chim. Acta **19,** L45 (1976)

[64] S G Popov and V A Levitskii, Russ. J. Phys. Chem. **55,** 46 (1981)

[65] M S Shubin, A O Litinskii, G P Popov and A N Men, Zh. Strukt. Khim. **17,** 160 (1976)

[66] H D Lutz, W Schmidt and H Haeusler, J. Phys. Chem. Solids **42,** 287 (1981)

[67] R Kanno, Y Takeda and O Yamamoto, Mater. Res. Bull. **16,** 999 (1981)

[68] C Cros, L Hanebali, L Latié, G Villeneuve and G Wang, Solid State Ionics **9/10,** 139 (1983)

[69] W Schmidt and H D Lutz, Ber. Bunsenges. Phys. Chem. **88,** 720 (1984)

[70] R Kanno, Y Takeda, K Takada and O Yamamoto, J. Electrochem. Soc. **131-3,** 469 (1984)

[71] C Cros, W Gang, J L Soubeyroux, P Hagenmuller. R Kanno and O Yamamoto, Trans.-Struct. Relat. Fast Ion Mixed Cond., 6th Proc. Risoe Int. Symp. Metall. Mater. Sci. 221 (1985)

[72] C J Chen, M Greenblatt and J V Waszczak, Mater. Res. Bull. **21,** 609 (1986)

[73] C J Chen, M Greenblatt and J V Waszczak, Solid State Ionics **18/19,** 838 (1986)

[74] J C Hunter, J. Solid State Chem. **39,** 142 (1981)

[75] A Mosbah, A Verbaere and M Tournoux, Mater. Res. Bull. **18,** 1375 (1983)

[76] M M Thackeray, P J Johnson, L A de Picciotto, P G Bruce and J B Goodenough, Mater. Res. Bull. **19,** 179 (1984)

[77] D W Murphy, M Greenblatt, S M Zahurak, R J Cava, J V Waszczak, G W Hull and R S Hutton, Rev. Chim. Minér. **19,** 441 (1982)

[78] D W Murphy, R J Cava, S M Zahurak and A Santoro, Solid State Ionics, **9/10,** 413 (1983)

[79] B Krutzsch and S Kemmler-Sack, J. Less-Common Metals, **124,** 111 (1986)

[80] B Krutzsch and S Kemmler-Sack, J. Less-Common Metals, **124,** 155 (1986)

[81] M M Thackeray, L A de Picciotto, A de Kock, P J Johnson, V A Nicholas and K T Adendorff, J. Power Sources **21,** 1 (1987)

[82] D W Murphy, P A Christian, F J Di Salvo and J N Carides, J. Electrochem. Soc. **126,** 497 (1979)

[83] K West, B Zachau-Christiansen, M J Landeira and T Jacobsen, 6th Proc. Risoe Int. Symp. Metall. Mater. Sci., 265 (1985)

[84] K West, B Zachau-Christiansen, M J L Østergard and T Jacobsen, J. Power Sources **20,** 165 (1987)

[85] A Tranchant, R Messina and J Perichon, J. Electroanal. Chem. **113,** 225 (1980)

[86] K West, T Jacobsen, B Zachau-Christiansen and S Atlung, Electrochimica Acta **28,** 97 (1983)

[87] N C Chaklanabish and H S Maiti, J. Power Sources **16,** 97 (1985)

[88] K Wiesener, W Schneider, D Ilić, K H Hallmeier and E Brackmann, J. Power Sources **20,** 157 (1987)

[89] K M Abraham, J L Goldman and M D Dempsey, J. Electrochem. Soc. **128,** 2493 (1981)

[90] K West, B Zachau-Christiansen and T Jacobsen, Electrochimica Acta **28,** 1829 (1983)

[91] B C Tofield, R M Dell, J Jansen, EUR Report 9236 Energy Conserv. Ind., Vol. 2, p 198 (1984)

[92] K West, B Zachau-Christiansen, T Jacobsen and S Atlung, J. Power Sources **14,** 235 (1985)

[93] G Pistoia, F Rodante and M Tocci, Solid State Ionics **20,** 25 (1986)

[94] B Zachau-Christiansen, K West and T Jacobsen, Mater. Res. Bull. **20,** 485 (1985)

[95] G Pistoia, S Panero, M Tocci, R V Moshtev and V Manev, Solid State Ionics **13,** 311 (1984)

[96] G Pistoia, M Pasquali, M Tocci, R V Moshtev and V Manev, J. Electrochem. Soc. **132,** 281 (1985)

[97] G Pistoia, M Pasquali, M Tocci, V Manev and R V Moshtev, J. Power Sources **15,** 13 (1985)

[98] M Pasquali, G Pistoia, V Manev and R V Moshtev, J. Electrochem. Soc. **133,** 2454 (1986)

[99] G Pistoia, M L Di Vona and P Tagliatesta, Solid State Ionics **24,** 103 (1987)

[100] J C Hunter and F B Tudron, Proc. Electrochem. Soc. **85-4,** 444 (1985)

[101] W I F David, M M Thackeray, P G Bruce and J B Goodenough, Mater. Res. Bull. **19,** 99 (1984)

[102] J B Goodenough, M M Thackeray, W I F David and P G Bruce, Rev. Chim. Minér. **21,** 435 (1984)

[103] International Tables for X-Ray Crystallography, Vol 3, Kynoch Press, Birmingham (1962)

[104] B D Cullity, Elements of X-ray diffraction, Second ed., Addison-Wesley, Reading (Massachussettes) (1978)

[105] S Atlung, K West and T Jacobsen, J. Electrochem. Soc. **126,** 1311 (1979)

[106] E Peled, J. Electrochem. Soc. **126,** 2047 (1979)

[107] W Peukert, Elektrotechn. Z. **18,** 287 (1897)

[108] R Messina, J Perichon, M Broussely and G Gerbier, J. Appl. Electrochem. **8,** 87 (1978)

[109] R Messina, J Perichon, M Broussely and G Gerbier, J. Appl. Electrochem. **8,** 405 (1978)

[110] R Fournie, R Messina and J Perichon, J. Appl. Electrochem. **9,** 329 (1979)

[111] M Zanini, J. Electrochem. Soc. **132,** 588 (1985)

[112] R S Nicholson and I Shein, Anal. Chem. **36,** 706 (1964)

[113] J R Dahn and R R Haering, Solid State Ionics **2,** 19 (1981)

[114] M Armand, F Dalard, D Deroo and C Mouliom, Solid State Ionics **15,** 205 (1985)

[115] G Barral, J P Diard and C Montella, Electrochimica Acta **30,** 585 (1985)

[116] S Basu and W L Worrell, in : Fast Ion Transport in Solids (North-Holland, Amsterdam, 1981) 363

[117] A Honders, E W A Young, A H van Heeren, J H W de Wit and G H J Broers, Solid State Ionics **9/10,** 375 (1983)

[118] M Ottaviani, S Panero, S Morzilli and B Scrosati, Solid State Ionics **20,** 197 (1986)

[119] W Weppner and R A Huggins, J. Electrochem. Soc. **124,** 1569 (1977)

[120] W Weppner and R A Huggins, Ann. Rev. Mater. Sci. **8,** 269 (1978)

[121] G J Dudley and B C H Steele, J. Solid State Chem. **31,** 233 (1980)

[122] A Honders and G H J Broers, Solid State Ionics **15,** 173 (1985)

[123] M J Smith and C A Vincent, Electrochimica Acta **30,** 931 (1985)

[124] P C Spurdens and B C H Steele, Solid State Ionics **21,** 151 (1986)

[125] A Honders, J M der Kinderen, A H van Heeren, J H W de Wit and G H J Broers, Solid State Ionics **15,** 265 (1985)

[126] M S Whittingham and M B Dine Electrochem. Soc. **124,** 1387 (1977)

[127] I Bernal and G Fraenkel, J. Amer. Chem. Soc. **86,** 1761 (1964)

[128] M Salomon and E J Plichta, Electrochimica Acta **30,** 113 (1985)

[129] P J Wiseman, D. Phil. Thesis, University of Oxford, 1974

[130] D W Murphy, J N Carides, C Cros, F J Di Salvo and J V Waszczak, Mater. Res. Bull. **12,** 125 (1977)

[131] P G Dickens, S J French, A T Hight and M F Pye, Mater. Res. Bull. **14,** 1295 (1979)

[132] D W Murphy, P A Christian, J N Carides and F J Di Salvo in P Vashista, J N Mundy and G K Shenoy (eds), Fast Ion Transport in Solids, p 137, North Holland (1979)

[133] K Vidyasagar and J Gopalakrishnan, J. Solid State Chem. **42,** 217 (1982)

[134] W Rüdorff and H Becker, Z. für Naturforsch. **9B,** 614 (1954)

[135] M M Thackeray, L A de Picciotto, W I F David, P G Bruce and J B Goodenough, J. Solid State Chem. **67,** 285 (1987)

[136] F A Cotton and G Wilkinson, "Advanced Inorganic Chemistry", 3rd ed., Interscience, New York (1972)

[137] K Mizushima, M Tanaka, A Asai, S Iida and J B Goodenough, J. Phys. Chem. Solids **40,** 1129 (1979)

[138] R D Shannon, Acta Crystallogr. **A32,** 751 (1976)

[139] G Colsmann, W Dahmcke, L Schütte and B Reuter, Z. Anorg. Allgem. Chem. **456,** 61 (1979)

[140] L A de Picciotto, unpublished results

[141] S Kikkawa, S Miyazaki and M Koizumi, J. Power Sources **14,** 231 (1985)

[142] K Mizushima, P C Jones, P J Wiseman and J B Goodenough, Solid State Ionics **3/4,** 171 (1981)

[143] M G S R Thomas, P G Bruce and J B Goodenough, J. Electrochem. Soc. **132,** 1521 (1985)

[144] B Buffat, G Demazeau, M Pouchard, J M Dance and P Hagenmuller, J. Solid State Chem. **50,** 33 (1983)

[145] M G S R Thomas, W I F David, J B Goodenough and P Groves, Mater. Res. Bull. **20,** 1137 (1985)

[146] C Delmas, J -J Braconnier, A Maazaz and P Hagenmuller, Rev. Chim. Minér. **19,** 343 (1982)

[147] B Reuter and J Jaskowsky, Angew. Chem. **72,** 209 (1960)

[148] H Kessler and M J Sienko, J. Chem. Phys. **55,** 5414 (1971)

[149] D Arndt, K Müller, B Reuter and E Riedel, J. Solid State Chem. **10,** 270 (1974)

[150] E Pollert, Krist. Tech. **6,** K25 (1971)

[151] Reuter and J Jaskowsky, Ber. Bunsenges. Phys. Chemie **70,** 189 (1966)

[152] A.S.T.M. Powder Diffraction File 18-736

[153] A.S.T.M. Powder Diffraction File 26-1199

[154] A.S.T.M. Powder Diffraction File 19-629

[155] A.S.T.M. Powder Diffraction File 22-1084

[156] A.S.T.M. Powder Diffraction File 17-115

[157] A Rousset, B Chassagneux and B Gillot, Ann. Chim. Fr. **8,** 227 (1983)

[158] J C Joubert, Bull. Soc. Fr. Mineral. Cristallogr. **90,** 598 (1967)

[159] G A Steigmann, H H Sutherland and J Goodyear, Acta Crystallogr. **19,** 967 (1965)

[160] W Laqua, S Dudda and B Reuter, Mater. Res. Bull. **19,** 339 (1984)

[161] Chem. Abstr. **86,** 11373a (1977)

[162] M Maazaz, PhD Thesis, University of Bordeaux (1982), p 18

[163] W I F David, M M Thackeray, L A de Picciotto and J B Goodenough, J. Solid State Chem. **67,** 316 (1987)

[164] R J Cava, D W Murphy, S M Zahurak, A Santoro and R S Roth, J. Solid State Chem. **53,** 64 (1984)

[165] A Manthiram and J B Goodenough, Can. J. Phys. **65,** 1309 (1987)

[166] K Aoki, K Tokuda and H Matsuda, J. Electroanal. Chem. **146,** 417 (1983)

[167] D B Rogers, J L Gillson and T E Gier, Solid State Commun. **5,** 263 (1967)

[168] L Schütte, G Colsmann and B Reuter, J. Solid State Chem. **21,** 227 (1979)

[169] P J Johnson, unpublished results (this laboratory)

[170] A Mendiboure, C Delmas and P Hagenmuller, J. Solid State Chem. **57,** 323 (1985)

[171] T Armbruster and G A Lager, J. Phys. Chem. Solids **42,** 725 (1981)

[172] W I F David, J B Goodenough, M M Thackeray and M G S R Thomas, Rev. Chim. Minér. **20,** 636 (1983)

[173] V A Nicholas and L A de Picciotto, unpublished results

[174] L A de Picciotto and M M Thackeray, Extended Abstracts, 6th Int. Conf. Solid State Ionics, Garmisch-Partenkirchen (West Germany) 475 (1987)

[175] B Reuter, Bull. Soc. Chim. France **4,** 1053 (1965)

[176] D B Rogers, J B Goodenough and A Wold, J. Appl. Phys. **35,** 1069 (1964)

[177] B Reuter and K Müller, Z. Anorg. Allgem. Chem. **368,** 174 (1969)

[178] D Arndt, Dissertation, TU-Berlin (1972)

[179] B Reuter and K Müller, Naturw. **54,** 164 (1967)

[180] B Reuter and G Colsmann, Z. Anorg. Allgem. Chem. **394,** 138 (1972)

[181] J -C Joubert and A Durif, Comptes Rendus **256,** 4403 (1963)

[182] M Born and J E Mayer, Z. Phys. **75,** 1 (1932)

[183] M Born and K Huang, "Dynamical Theory of Crystal Lattices", Oxford University Press, London and New York (1954)

[184] E Madelung, Z. Phys. **19,** 524 (1918)

[185] M P Tosi, Solid State Physics **16,** 1 (1964)

[186] W Van Gool and A G Piken, J. Mater. Sci. **4,** 95 (1969)

[187] H M Evjen, Phys. Rev. **39,** 675 (1932)

[188] P P Ewald, Ann. Physik **64,** 253 (1921)

[189] J Dahl, J. Phys. Chem. Solids **26,** 33 (1965)

[190] F Bertaut, J Phys. Radium **13,** 499 (1952)

[191] B R A Nijboer and F W De Wette, Physica **23,** 309 (1957)

[192] F W De Wette and G E Schacher, Phys. Rev. **137,** A78 (1965)

[193] F W De Wette and G E Schacher, Phys. Rev. **137,** A92 (1965)

[194] V Massidda, Physica **85B,** 311 (1977)

[195] C A Sholl, Proc. Phys. Soc. **87,** 897 (1966)

[196] C A Sholl, Proc. Phys. Soc. **92,** 434 (1967)

[197] V Massidda, Physica **95B,** 317 (1978)

[198] V Massidda and J A Hernando, Physica **101B,** 159 (1980)

[199] R Fischer and H Ludviczek, Monatsh. Chem. **106,** 223 (1975)

[200] S G Popov and V A Levitskii, Russ. J. Phys. Chem. **57,** 530 (1983)

[201] S G Popov and V A Levitskii, Russian J. Phys. Chem. **55,** 49 (1981)

[202] S G Popov and V A Levitskii, Russian J. Phys. Chem. **55,** 647 (1981)

[203] F de Boer, J H van Santen and E J W Verwey, J. Chem. Phys. **18,** 1032 (1950)

[204] J A Hernando and V Massidda, Comput. Phys. Commun. **22,** 13 (1981)

[205] J A Hernando and V Massidda, Comput. Phys. Commun. **25,** 111 (1982)

[206] K Satomi, J. Phys. Soc. Japan **16,** 258 (1961)

[207] Zahlenwerte und Funktionen aus Naturwissenschaften und Technik, Vol. 7b, Landolt-Bornstein, Springer Verlag, Berlin (1975)

[208] International Tables for X-Ray Crystallography, Vol 1, Kynoch Press, Birmingham (1952)

[209] P G Dickens, S J French, A T Hight, M F Pye and G J Reynolds, Solid State Ionics **2,** 27 (1981)

[210] P G Dickens and G J Reynolds, Solid State Ionics **5,** 331 (1981)

[211] K H Cheng and M S Whittingham, Solid State Ionics **1,** 151 (1980)

[212] G S Hammond, J. Am. Chem. Soc. **77,** 334 (1955)

[213] S C Parker, Solid State Ionics **8,** 179 (1983)

[214] C Chieh, B L Chamberland and A F Wells, Acta Cryst. B**37,** 1813 (1981)

[215] L A de Picciotto, M Pasquali, G Pistoia and M M Thackeray, Extended Abstracts, 6th Int. Conf. Solid State Ionics, Garmisch-Partenkirchen (West Germany), 623 (1987)

[216] G Pistoia, M Pasquali, L A de Picciotto and M M Thackeray, Solid State Ionics (1988). In press

[217] G Pistoia, private communication

[218] J B Goodenough, private communication